



## Identification of autism spectrum disorder based on electroencephalography: A systematic review

Jing Li<sup>a,1</sup>, Xiaoli Kong<sup>a,1</sup>, Linlin Sun<sup>b,c</sup>, Xu Chen<sup>d,e</sup>, Gaoxiang Ouyang<sup>f,\*</sup>, Xiaoli Li<sup>f</sup>, Shengyong Chen<sup>a</sup>

<sup>a</sup> School of Computer Science and Engineering, Tianjin University of Technology, Tianjin, 300384, China

<sup>b</sup> Neuroscience Research Institute, Peking University, Beijing, 100191, China

<sup>c</sup> Key Laboratory for Neuroscience, Ministry of Education/National Health Commission of China, Beijing, 100191, China

<sup>d</sup> The National Clinical Research Center for Mental Disorders & Beijing Key Laboratory of Mental Disorders, Beijing Anding Hospital, Beijing, 100120, China

<sup>e</sup> The Advanced Innovation Center for Human Brain Protection, Capital Medical University, Beijing, 100032, China

<sup>f</sup> State Key Laboratory of Cognitive Neuroscience and Learning, Beijing Normal University, Beijing, 100875, China



### ARTICLE INFO

#### Keywords:

Autism spectrum disorder  
Electroencephalography  
Machine learning  
Deep learning  
Multi-model fusion

### ABSTRACT

Autism Spectrum Disorder (ASD) is a neurodevelopmental disorder characterized by difficulties in social communication and repetitive and stereotyped behaviors. According to the World Health Organization, about 1 in 100 children worldwide has autism. With the global prevalence of ASD, timely and accurate diagnosis has been essential in enhancing the intervention effectiveness for ASD children. Traditional ASD diagnostic methods rely on clinical observations and behavioral assessment, with the disadvantages of time-consuming and lack of objective biological indicators. Therefore, automated diagnostic methods based on machine learning and deep learning technologies have emerged and become significant since they can achieve more objective, efficient, and accurate ASD diagnosis. Electroencephalography (EEG) is an electrophysiological monitoring method that records changes in brain spontaneous potential activity, which is of great significance for identifying ASD children. By analyzing EEG data, it is possible to detect abnormal synchronous neuronal activity of ASD children. This paper gives a comprehensive review of the EEG-based ASD identification using traditional machine learning methods and deep learning approaches, including their merits and potential pitfalls. Additionally, it highlights the challenges and the opportunities ahead in search of more effective and efficient methods to automatically diagnose autism based on EEG signals, which aims to facilitate automated ASD identification.

### 1. Introduction

Autism spectrum disorder (ASD) is a heterogeneous neurodevelopmental disorder with core symptoms of social communication, restricted or repetitive behaviors, or a narrow range of interests or activities [1]. A growing body of epidemiological and preclinical evidence indicated that the etiology of ASD is due to a complex interaction between genetic and environmental factors such as maternal immune activation during pregnancy [2]. Although ASD is considered as a lifelong disability, with timely treatment, the developmental quotients, cognitive abilities and language skills of ASD children can be improved to a large extent [3]. A recent study [4] of quantifying longitudinal changes in ASD core symptoms found that the outcome is significantly

correlated with early diagnosis, and the interventions of younger ASD children can be benefited with greater brain plasticity and behavioral flexibility. Therefore, early diagnosis and intervention of ASD children are with great significance to the rehabilitation of ASD children [5]. At present, the clinical diagnosis of ASD mainly relies on the evaluation of professional doctors according to childhood autism rating scale, 2nd edition (CARS2) [6], autism behavior checklist (ABC), autism diagnostic observation schedule, 2nd edition (ADOS-2) [7], checklist for autism in toddlers (CHAT) [8], autism diagnostic interview revised (ADI-R) [9], etc. However, the evaluation process is cumbersome and requires high professional ability and clinical experience of doctors, causing most ASD children are not diagnosed in time, thus missing the golden period of intervention. With the development of machine learning techniques,

\* Corresponding author.

E-mail address: [ouyang@bnu.edu.cn](mailto:ouyang@bnu.edu.cn) (G. Ouyang).

<sup>1</sup> These authors contributed equally to this work.

researchers began to diagnose ASD automatically by extracting behavioral or brain features through different feature extractors and classifiers, which can effectively reduce the complexity of disease diagnosis, meanwhile provide more objective and accurate diagnosis.

Over the past decade, numerous autism diagnosis methods have been proposed based on machine learning. ASD children show a variety of behavioral disorders [26], including improper or missing gait, eye movement, facial expressions, hand gestures, and language [27], therefore behavioral characteristics can be analyzed by machine learning techniques to distinguish ASD children from typically developing (TD) through facial expressions recognition [10,11], gaze analysis on the regions of interest [12,13], eye movement analysis [14,15], gait recognition [16,17], hand gesture recognition [18,19] and assessment of response-to-instructions/name [20,21]. However, the diagnosis based on appearance can only explore the extrinsic behavior of ASD, but ignores the intrinsic neural mechanism of ASD. By contrast, brain imagings such as EEG [22,23] and fMRI [24,25] can reveal the heterogeneity of autism. From the biological perspective, ASD children typically suffer from increased brain size [28], disorganization of white and gray matter [29] and abnormalities in gyral cortical anatomy [30]. Therefore, EEG and fMRI are very important for the diagnosis of ASD. The fMRI is an imaging technology relying on blood oxygenation level-dependent (BOLD), which reflects the level of local cerebral blood flow/oxygenation and is an indirect method to assess neural activity [31]. Wen et al. [32] proposed a prior brain structure learning-guided multi-view graph convolution network to successfully implement fMRI-based autism diagnosis. However, the fMRI scanner is bulky, immobile, and expensive, which limits the acquisition environment to specific hospitals.

Electroencephalography (EEG) records the electrical wave activity of nerve cells in the cerebral cortex when groups of neurons fire synchronously [37]. Compared with fMRI, the EEG recordings are with high temporal resolution, and easy to acquire from different age groups and different developmental levels [34]. At present, EEG decoding techniques are becoming more and more sophisticated. Wang et al. [35] proposed a sparse Bayesian learning-based EEG decoding algorithm that provides a novel EEG-tailored machine learning tool for decoding brain activity. Raziani et al. [36] proposed an efficient hybrid model based on modified whale optimization algorithm and multilayer perceptron neural network, which is effectively used for medical classification problems such as EEG decoding and ASD identification. Numerous studies have shown that EEG has become an effective tool for brain-computer interface (BCI), emotion recognition [38–40], mental workload detection [41], seizure detection [42] and ASD diagnosis. As the EEG can directly measure the electrical activity of the central nervous system [33], changes in brain activity caused by emotional changes or neurological diseases such as ASD can be observed by comparing EEG signals with the control group. For example, ASD children often suffer from paroxysmal EEG abnormalities [43], mirror neuron system dysfunction [44], reduced long-term and short-term coherence between brain regions, local hyperconnectivity [45]. Many researches [46–48] demonstrated that EEG can provide reliable biomarkers for ASD diagnosis, enhance diagnostic objectivity and reduce misdiagnosis, thus enabling more accurate diagnosis and timely intervention. At the same time, EEG-based diagnosis can provide more personalized intervention based on the analysis of heterogeneous neurophysiological characteristics of autistic patients.

In the past decade, traditional machine learning and deep learning techniques have been widely used for ASD diagnosis based on EEG recordings. Both of the methods require data pre-processing, including referencing, downsampling, de-artifacting, etc. Traditional machine learning methods manually extract features through time-domain analysis, frequency-domain analysis, or time-frequency domain analysis, and then use classifiers such as support vector machines (SVM) [140] and multilayer perceptron (MLP) [145] to train the model. Deep learning models, e.g., convolutional neural network and graph convolution network, possess strong representational power and can

automatically extract features from EEG data and identify ASD. Currently, deep learning is considered to be one of the most promising techniques, but traditional machine learning-based ASD identification methods still occupy a significant position. The choice of a specific method should be considered comprehensively based on the dataset scale, problem complexity, and the need for model interpretability. Generally, traditional machine learning methods are suitable for small sample sizes of data and high requirements on model interpretability. Deep learning methods perform well in dealing with large-scale datasets and exploring complex relationships among the features. Therefore, in this review, we summarize both machine learning and deep learning methods.

To the best of our knowledge, there are four reviews [1,49–51] that describe machine learning methods for studying ASD. However, the summary of the latest traditional machine learning methods and deep learning techniques for autism diagnosis is still incomplete. In order to facilitate researchers to better understand the research progress of EEG-based ASD identification and stimulate new ideas, it is necessary to review the recent research. This review differs from them as shown in Table 1. Brihadiswaran et al. [1] introduced traditional machine learning approaches for EEG-based autism diagnosis from 2010 to 2018. Khodatars et al. [49] reviewed deep learning studies using brain imaging data such as EEG and MRI for the diagnosis and rehabilitation of autism, including CNNs, self-encoders and RNNs. These are similar to our summarizing machine learning methods for ASD identification using EEG signals, enabling researchers to understand the research progress in the field. Meanwhile, we complement it with the latest conventional machine learning algorithms, more recent deep learning algorithms, and multimodal fusion algorithms for EEG, eye tracking, and facial expression. In addition, the challenges and future research directions in the field of EEG-based ASD identification are discussed. Parlett-Pelleriti et al. [50] reviewed the unsupervised machine learning methods in ASD research, e.g., K-means clustering, hierarchical clustering, model-based clustering, and self-organizing maps. The review includes a wide range of studies such as ASD classification based on a variety of data and gene expression of ASD. By contrast, our review explores traditional machine learning and deep learning algorithms for ASD identification based on EEG signals. Das et al. [51] summarized the traditional machine learning and deep learning approaches for analyzing EEG and magnetoencephalography data of ASD subjects, including SVM, KNN, ANN, and CNN. The review categorized all the literatures according to the age group of the ASD subjects and summarized different methods of ASD identification. On the contrary, our review categorizes and summarizes representative methods of traditional machine learning (e.g., SVM, random forest, MLP, KNN, and logistic regression) and recent deep learning (e.g., CNN, RNN, GCN, and AE) approaches based on EEG recordings, which leads to a clearer structure and helps the readers understand the strengths and weaknesses of different methods. The contributions of this review are as follows:

1. This review covers the recent literatures in EEG-based automatic diagnosis of autism, exploring recent research advances in machine learning and deep learning methods;
2. The process of machine learning for EEG-based ASD identification, including data preprocessing, feature extraction and classification, is described to help readers clearly understand the strengths and limitations of each method;
3. Deep learning methods for EEG-based ASD identification, involving CNN-based models, RNN-based models, and GCN-based models, are presented. A comprehensive overview and insights are provided for network model construction;
4. Methods for ASD identification using multimodal data are presented, including combining EEG with eye movement, and facial expression. Multimodal fusion algorithms and their effectiveness in ASD identification are discussed; and

**Table 1**

Differences between this review and other related reviews. CNN: Convolutional Neural Network, AE: Autoencoder, RNN: Recurrent Neural Network, GCN: Graph Convolutional Network.

Review	Time Span	Dataset	Task	Method			
				Data Preprocessing	Feature Extraction	Machine Learning	Deep Learning
Brihadiswaran et al. [1]	2010 to 2018	EEG	ASD Identification	✓	✓	✓	✗
Khodatars et al. [49]	2016 to 2020	MRI, EEG	ASD Identification and Rehabilitation	✓	✗	✗	CNN, AE, RNN
Parlett-Pelleriti et al. [50]	2000 to 2021	Behavioral Data, Biomedical Data, Genetic Data	ASD Identification, Gene Expression, Behavioral Prediction	✗	✗	✓	✗
Das et al. [51]	2011- to 2022	EEG, ECG	ASD Identification	✗	✗	✓	CNN
Ours	2010 to 2023	EEG	ASD Identification	✓	✓	✓	CNN, RNN, GCN, Multi-modal Fusion

5. The challenges and future directions of EEG-based ASD identification are discussed, providing useful guidance for early identification of ASD in the future research.

In this review, a systematic search of related publications was performed using the four stages (i.e., identification, screening, eligibility, and included) of the Preferred Reporting Items for Systematic Reviews and Meta-Analyses (PRISMA) [52] statement. At the stage of identification, we searched the Google Scholar, SpringerLink, and IEEE Explorer databases to explore the papers published from January 1, 2010 to the present using the keywords “autism”, “ASD”, “electroencephalogram”, “EEG”, “machine learning”, “deep learning”, “identification”, “diagnosis” and “classification”. After that, the search was narrowed down according to the steps of “Screening”, “Eligibility”, and “Included”, respectively. Fig. 1 gives the flowchart of our search method. Finally, 76 studies met the above criteria and were included in this review.

The remainder of this paper is organized as follows: Section 2 summarizes representative EEG datasets for autism identification and commonly used assessment metrics. Section 3 reviews traditional machine learning methods, including data preprocessing, feature extraction and classification. Section 4 outlines deep learning methods, including convolutional neural network-based, recurrent neural network-based and graph convolutional network-based models for autism identification. Section 5 describes multimodal fusion methods based on EEG, eye tracking and facial expression. Section 6 discusses current challenges and opportunities for EEG signal-based ASD identification.

## 2. EEG-based ASD datasets and evaluation metrics

### 2.1. Datasets

Due to the complexity of biomedical data and the privacy of health information on children, there are only few publicly available datasets that can be used to analyze EEG differences between children with autism and normally developing children. To the best of our knowledge, there is only one publicly available EEG dataset for autism identification. This dataset is provided by Brain Computer Interface Group of King Abdulaziz University (KAU), Jeddah, Saudi Arabia, (<http://malhaddad.kau.edu.sa/Pages-BCI-Datasets.aspx>). It consists of EEG recordings from 8 autistic boys (aged from 10 to 16 years) and 10 typically developing boys (aged from 9 to 16 years). These resting-state EEG signals were recorded at a sampling rate of 256 Hz using a 16-channel EEG data acquisition system consisting of a g. tec EEGcap, 16 Ag/AgCl electrodes, a g. tec GAMMABox, a g. tec USBamp and a BCI2000. During the recording, the data were filtered using a band-pass filter with a frequency band (0.1–60) Hz. Some research teams independently recruited ASD children and TD children to establish datasets that can be used to validate the effectiveness of ASD identification methods, but these datasets are usually not publicly available since they often involve sensitive personal information about the participants. Table 2 demonstrates the representative EEG datasets for ASD identification, which provides the information of the number of subjects, the age, the number of electrodes, sampling rate, and duration of the EEG signals, as well as whether they are publicly available or not.

### 2.2. Evaluation metrics

Model evaluation is important to assess autism identification models. Its main purpose is to validate the feasibility, accuracy and generalization ability of the proposed method in practical applications. For the task of autism identification, commonly used evaluation metrics include accuracy, specificity, sensitivity, precision, F1 Scores and area under curve (AUC).

True positive (TP) denotes the number of correctly classified positive samples. True negative (TN) represents the number of correctly classified negative samples. False positive (FP) denotes the number of samples incorrectly classified as positive. False negative (FN) denotes the number of samples incorrectly classified as negative. The commonly used evaluation metrics are given as follows:

- Accuracy represents the ratio of the number of correctly categorized samples to the total number of samples in the dataset. It is a fundamental metric widely used in the studies of disease diagnosis. The accuracy score ranges between 0 and 1, where a score of 1 indicates that all positive and negative samples are correctly classified, while a

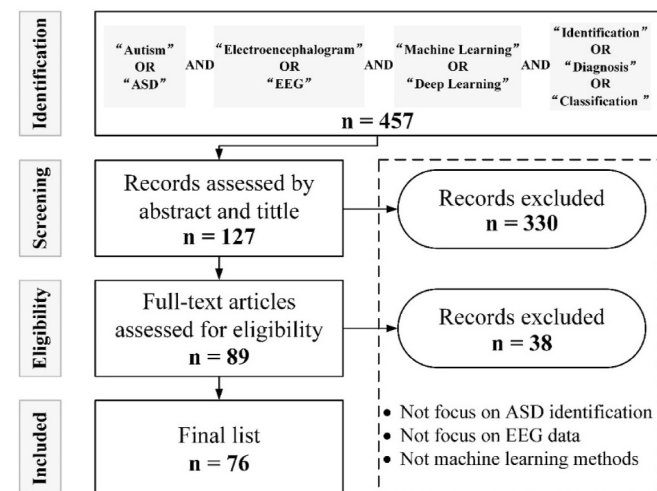


Fig. 1. Flowchart of our search method based on the PRISMA statement [52].

**Table 2**

The EEG-based ASD datasets. HRA: High risk for ASD, LRC: Low risk for control.

Dataset	Subjects (ASD vs. TD)	Age (Year)	Channels	Sampling Rate (Hz)	Duration (s)	Publicly-Available (Yes/No)	Link
Alhaddad et al. [53] 2012	8 vs. 10	9 to 16	16	256	300–2400	Yes	<a href="https://malhaddad.kau.edu.sa/Page_s-BCI-Datasets.aspx">https://malhaddad.kau.edu.sa/Page_s-BCI-Datasets.aspx</a>
Ahmadi et al. [54] 2012	9 vs. 9	7 to 13	19	256	39	No	<a href="https://doi.org/10.1016/j.jneumeth.2012.08.020">https://doi.org/10.1016/j.jneumeth.2012.08.020</a>
Bosl et al. [48] 2013	46 (HRA) vs. 33 (TD)	0.5 to 2	64	256	20	No	<a href="https://doi.org/10.1186/1741-7015-9-18">https://doi.org/10.1186/1741-7015-9-18</a>
Peters et al. [45] 2013	16 vs. 46	2 to 5	19	256	439	No	<a href="https://doi.org/10.1186/1741-7015-11-54">https://doi.org/10.1186/1741-7015-11-54</a>
Bosl et al. [55] 2018	99 (HRA) vs. 89 (LRC)	0.25 to 3	19	256	30	No	<a href="https://doi.org/10.1038/s41598-018-24318-x">https://doi.org/10.1038/s41598-018-24318-x</a>
Kang et al. [107] 2018	52 vs. 52	4.54 ± 0.5 4.52 ± 0.67	19	1000	600	No	<a href="https://doi.org/10.1016/j.jocn.2018.06.049">https://doi.org/10.1016/j.jocn.2018.06.049</a>
Baygin et al. [179] 2021	61 vs. 61	4 to 13	64	500	15	No	<a href="https://doi.org/10.1016/j.combiomed.2021.104548">https://doi.org/10.1016/j.combiomed.2021.104548</a>
Dong et al. [169] 2021	86 vs. 98	3 to 6	8	1000	4	No	<a href="https://doi.org/10.1016/j.neucom.2021.04.009">https://doi.org/10.1016/j.neucom.2021.04.009</a>
Li et al. [150] 2022	95 vs. 91	>18	64	2048	600	No	<a href="https://doi.org/10.1038/s41598-022-22597-z">https://doi.org/10.1038/s41598-022-22597-z</a>
Wadhura et al. [100] 2023	30 vs. 30	5 to 21	8	250	–	No	<a href="https://doi.org/10.1109/JBHI.2022.3232550">https://doi.org/10.1109/JBHI.2022.3232550</a>

score of 0 shows that none of the samples are correctly classified. It is defined by:

$$\text{Accuracy} = \frac{TP + TN}{TP + TN + FP + FN} \quad (1)$$

ii) Specificity, also known as the “True Negative Rate”, measures the model ability to correctly identify negative instances. It is calculated as the ratio of true negatives to the sum of true negatives and false positives. A higher specificity score indicates that the model performs better in identifying negative cases. Its definition is:

$$\text{Specificity} = \frac{TN}{TN + FP} \quad (2)$$

iii) Sensitivity, also named recall, is used to evaluate the model ability to correctly identify positive instances. It is calculated as the ratio of true positives to the sum of true positives and false negatives. A sensitivity score of 1 indicates that the model can effectively identify all the positive cases. The definition is given by:

$$\text{Sensitivity}(Recall) = \frac{TP}{TP + FN} \quad (3)$$

iv) Precision evaluates the accuracy of positive predictions made by the model. It is calculated as the ratio of true positives to the sum of true positives and false positives. Precision provides insight into the reliability of positive predictions. The definition is denoted as follows:

$$\text{Precision} = \frac{TP}{TP + FP} \quad (4)$$

v) The F1 score is the harmonic mean of precision and sensitivity. It provides a comprehensive assessment of a model’s performance and is suitable for tasks with unbalanced datasets. It ranges between 0 and 1, with a higher score indicating that the model performs better in terms of both precision and sensitivity. The definition is:

$$\text{F1 Score} = 2 * \frac{\text{Precision} * \text{Sensitivity}}{\text{Precision} + \text{Sensitivity}} = \frac{2 * TP}{2 * TP + FP + FN} \quad (5)$$

vi) The area under curve (AUC) is the area under the receiver operating characteristic (ROC) curve that depicts the trade-off between the true-positive rate against the false-positive rate at various threshold settings [129]. Thus, the AUC quantifies the overall performance of a model across all possible thresholds. The higher the AUC, the better the model’s ability to distinguish between positive and negative instances.

### 3. Traditional machine learning

Traditional machine learning methods have been widely applied to analyzing EEG signals for ASD identification [130,150], which mainly include the following three steps: i) data pre-processing; ii) feature extraction; and iii) classification. As shown in Fig. 2, raw EEG data are firstly down-sampled, re-referenced, and normalized according to actual needs, and the artifacts are removed as much as possible to improve the signal-to-noise ratio. Then, discriminative features are learnt from pre-processed data, e.g., time domain features, frequency domain features, and time-frequency domain features. Finally, an appropriate classifier is selected to automatically analyze and distinguish the samples into different categories, so as to achieve the children of ASD diagnosis.

#### 3.1. Data pre-processing

EEG is a conventional tool to diagnose brain diseases and brain function tests in clinical medicine. However, the EEG signal is non-stationary and weak, and is easily interfered by activities outside the brain, such as blinking of eyes, heartbeat, and facial muscle activities, which can produce useless information [57]. Therefore, raw EEG signals must undergo data preprocessing before the use for signal analysis. Pre-processing of EEG data generally includes downsampling, channel selection, bandpass filtering, removing bad segments, de-artifacting, and re-referencing. The roles of these operations are as follows:

- 1) Downsampling: It reduces the number of data points by sampling the EEG data, which helps decrease computational load and accelerates subsequent analysis.
- 2) Channel selection: It eliminates EEG channels that contain noise and redundant information, thus reducing overfitting and improving the accuracy and efficiency of autism diagnosis.

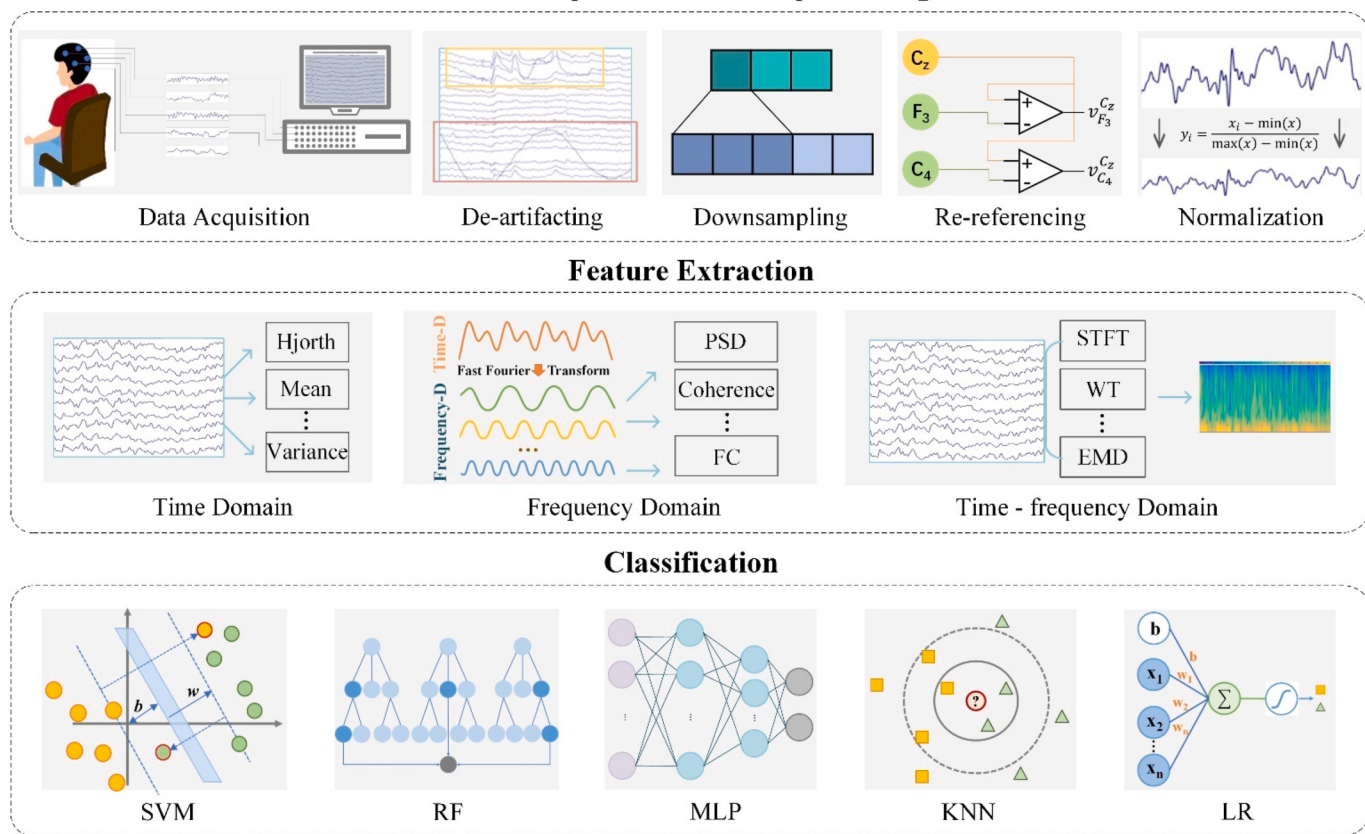


**Fig. 2.** Traditional machine learning methods for ASD identification based on EEG signals. PSD: power spectrum density [111], FC: functional connectivity [56], STFT: short-time Fourier transform [116], WT: wavelet transform [120], EMD: empirical mode decomposition [67], MLP: multilayer perceptron [145], SVM: support vector machines [140], KNN: K-nearest neighbors [146], RF: random forest [142], LR: logistic regression [148].

- 3) Bandpass filtering: It is used to limit EEG signals in a specific frequency range, thus reducing meaningless high and low frequency signals.
- 4) Removing bad EEG segments: Identifying and removing segments corrupted by motion artifacts, eye movements, or other disturbances ensures that the analysis is not significantly affected by apparent artifacts.
- 5) De-artifacting: Recognizing and correcting artifacts caused by eye movements, muscle activity, or other sources enables more accurate subsequent analysis.
- 6) Re-referencing: Altering the reference point of the EEG signal eliminates the influence of electrode placement and scalp shape, ensuring data consistency.

Among them, de-artifacting is the most important step of data pre-processing [60]. The reason is that eye blinks, muscle contractions, heartbeats, and devices often produce large and scattered physiological and non-physiological artifacts in EEG recordings [58]. The existence of a large number of artifacts seriously affects the extraction of useful information [59], and subsequently influences the ultimate diagnosis results of ASD.

### 3.1.1. De-artifacting

The EEG signal is a mixture of multiple sources and signal decomposition is required to obtain a pure EEG signal. As a blind source separation (BSS) technique [62], the independent component analysis (ICA) [61] is one of the most widely used methods for filtering artifacts from EEG signals. Different from traditional BSS techniques, ICA decomposes the raw EEG signal into a set of independent source signals [63] through an optimization algorithm [64]. Therefore, it can separate the EEG

signals from the artifacts and thus remove the artifacts. Fig. 3 gives the process of ICA. Here,  $Y = [y(1), y(2), \dots, y(p)]^T \in R^{p \times n}$  denotes  $p$  source signals;  $A = [a(1), a(2), \dots, a(m)] \in R^{m \times p}$  is the mixing matrix;  $W$  is a filtration matrix and the approximation of  $A^{-1}$ ,  $X = [x(1), x(2), \dots, x(m)] \in R^{m \times n}$  denotes the EEG signal with  $m$  channels;  $\hat{Y} = [\hat{y}(1), \hat{y}(2), \dots, \hat{y}(m)]^T \in R^{m \times n}$  is an approximation of  $Y$ ; and  $W^{-1}$  is the inverse of  $W$ .

In detail, the EEG signal  $X$  can be expressed as a mixture of multiple source signals:

$$X = AY \quad (6)$$

which represents the magnitude of each source signal for each EEG channel.

A full-rank factorization of the EEG signal  $X$  is performed to obtain the filtration matrix  $W$  in Eq. (7), which is measured by a cost function such as minima of Kullback-Leibler divergence or maximization of cumulants, so that the components of  $Y$  estimated by Eq. (8) are as independent as possible from each other [63].

$$W = A^{-1} \quad (7)$$

$$\hat{Y} = WX \quad (8)$$

where  $\hat{Y}$  denotes independent components.

Afterwards,  $\hat{Y}$  is visually examined or statistically calculated to select meaningful components of brainwave activity and to reject artifactual components. The selected independent components are remixed according to  $W^{-1}$  to obtain the reconstructed EEG signal.

Jung et al. [58] used ICA to remove artifacts in EEG signal. Firstly,

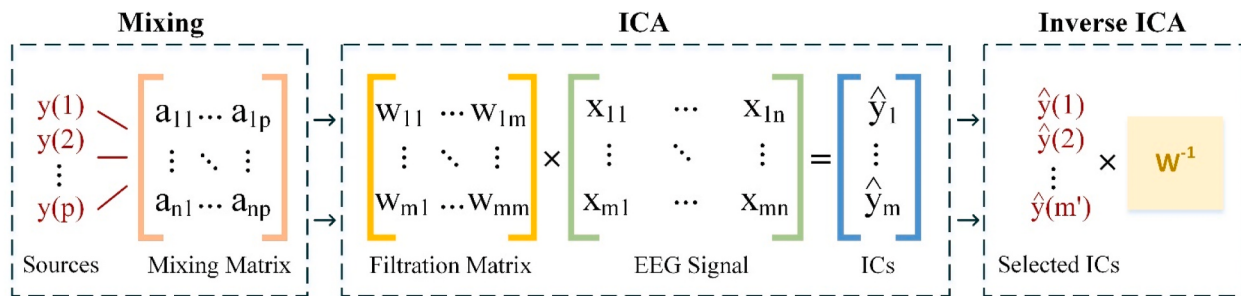


**Fig. 3.** Steps of the ICA and inverse ICA.

the multi-channel EEG signal is decomposed into spatially fixed and time-independent components. After eliminating spurious signal sources, a clean EEG signal is obtained. It was demonstrated that ICA is an effective and generally applicable method for EEG de-artifacting. The main disadvantage of this method is that it does not work well when the number of channels is lower or when there is limited EEG data available.

In addition, methods based on signal decomposition are also adopted for artifact filtering of EEG recordings. The basic idea is to decompose each individual channel into basic waveforms, remove waveforms containing artifacts, and reconstruct a clean EEG channel. For example, de-artifact by wavelet transform is to decompose the EEG signal with noise into multiple components in different frequency bands, which are represented by wavelet coefficients with different intensity distributions. Since the wavelet coefficients of the artifacts are smaller than those of the pure EEG signal [65], they can be effectively separated by setting an appropriate threshold. To be more specific, the wavelet coefficients greater than the threshold are considered to be generated by the EEG signal and retained, while the others are considered to be generated by artifacts and eliminated [66]. Moreover, there are some variants of signal decomposition methods. Iatsenko et al. [68] de-artifacted the EEG signal via nonlinear mode decomposition, which adaptively decomposes a raw EEG signal into a set of physically meaningful oscillations and removes the noise simultaneously. However, these traditional de-artifacting methods have obvious disadvantages, i.e., most methods require the recording of additional artifact channels or manual inspection to remove artifacts [69], leading to residual artifacts or information loss.

Deep learning can recognize artifacts more effectively, because it can adaptively learn the hidden features of neural oscillations in EEG signals, and better excavate the potential spatio-temporal dependencies in EEG signals. Zhang et al. [70] provided a large benchmark dataset for EEG de-artifacting, and trained four deep learning models, including fully connected neural networks [71], simple convolutional neural networks [153], 1D residual convolutional neural networks [72], and recurrent neural networks [73]. The experiment proved that the deep learning models can effectively remove the mixed myoelectric signals and oculoelectric signals in EEG signals. It is worth noting that this study only focused on the de-artifacting of 2s single-channel EEG epochs. In practical use, most of acquired raw EEG data are multi-channel signals longer than 2s. Therefore, it is necessary to design an effective deep learning-based de-artifacting method for multi-channel EEG signals with long duration. Narmada et al. [75] designed an adaptive artifacts wavelet denoising method based on deep learning. Firstly, the empirical mode decomposition technique is applied to decomposing the raw EEG data. Then, the decomposed signal is deeply de-artifacted using the discrete wavelet transform (DWT) and the CycleGAN [76]. At the same time, the hidden neurons in CycleGAN and parameters of DWT are adaptively optimized by opposing search elephant herding optimization. Finally, the artifact-removed signal is reconstructed using inverse DWT. However, the above-mentioned deep learning-based methods are still not effective to remove artifacts without a priori knowledge. Gao et al. [74] proposed a Dual-Scale CNN-LSTM model for deep artifact

removal, where dual-scale morphological features are extracted by dual-branch CNNs. Then, The long short-term memory (LSTM) [73] is used to learn the temporal dependencies from raw EEG signal, and its output is applied to reinforcing the dual-scale morphological features to highlight the differences between the artifacts and pure EEG signal. Finally, the artifacts are effectively identified, and the “desired” artifact-free EEG can be reconstructed via a fully connected layer.

### 3.1.2. The EEG pre-processing toolbox

We also introduce several popular toolboxes for pre-processing the EEG signals. After data acquisition, raw EEG data can be preprocessed by EEG pre-processing toolboxes [77]. Which can be used independently of the EEG acquisition system. Moreover, they have the advantages of convenience, high efficiency, and scalable functions, which makes them suitable for researchers without extensive programming ability or knowledge of EEG signal processing.

**EEGLAB** [78]: EEGLAB is an interactive Matlab toolbox developed by the Swartz Center for the Computational Neuroscience team at the University of California, USA. It can be used to process continuous and event-related electrophysiological data such as EEG, Magnetoencephalography (MEG), etc. EEGLAB includes data import, filtering techniques such as Independent Component Analysis (ICA) and artifact removal, time/frequency analysis, statistics of event-related information, and data visualization. In addition, users can also download other specific function plug-ins to expand the functions of the EEGLAB toolbox. EEGLAB has an easy-to-operate GUI interface that allows users to use commands and interactive operations to customize data processing, and can also call signal processing functions to write batch scripts. Many researchers prefer to utilize EEGLAB for data preprocessing due to its user-friendliness and convenience. However, it also has some limitations. For example, EEGLAB is a toolbox based on MATLAB, but most deep learning algorithms are written using the Python programming language. Therefore, it is inconvenient to preprocess data and construct models on different platforms.

**MNE** [79]: MNE is a python-based toolbox which provides comprehensive processing, analysis and visualization of neuroimaging data such as EEG and MEG, including source estimation, time-frequency analysis, and connectivity measures. The data processed by MNE can be used to train deep learning models without cross-platform. Therefore, the MNE toolbox has been widely used in EEG data preprocessing.

**FieldTrip** [80]: FieldTrip is a MATLAB-based EEG analysis toolbox. It has the capabilities of EEG source reconstruction that neither EEGLAB nor MNE has. However, it does not provide a GUI interface, and users need to call the function to implement EEG pre-processing.

### 3.2. Feature extraction

How to effectively analyze EEG signals has become the focus and difficulty to unravel the cognitive mechanism of human brain and identify brain diseases. Feature extraction is essential in characterizing the EEG signal, providing valuable information for ASD identification. Traditionally, various machine learning methods have been used to

extract features in different domains including time domain, frequency domain and time-frequency domain. Time-domain features provide information about the temporal dynamics of the EEG signal; the energy distribution in the frequency band is quantified by frequency-domain features; time-frequency domain features contain valuable information of both time-varying spectral content and temporal dynamics of brain activity. To achieve more accurate ASD identification, combinations of different methods are often used to capture various aspects of the EEG signal, but sometimes they also introduce redundant features. Therefore, the choice of feature extraction method depends on the specific research task and the characteristics of the EEG data.

### 3.2.1. Time-domain features

Time-domain EEG features are measured with respect to time, which are extracted from brain electrical activity over time by statistical algorithms. They are relatively simple and efficient to calculate, and can provide an intuitive interpretation of the temporal characteristics of the EEG signal. According to the number of channels involved in the feature extraction, time-domain EEG features can be mainly divided into three types, including single-channel features, dual-channel features and multi-channel features. The single-channel features are suitable for analyzing local brain activity, while the dual and multi-channel features are able to characterize the connectivity between brain regions and global dynamics.

#### A. Single-channel Features

The single-channel characteristics were obtained by calculating the EEG parameters independently for each electrode, and they capture brain activity in specific brain regions or electrodes, which is valuable for regional localization of abnormal brain activity. The features include statistical features such as mean, variance, standard deviation, skewness [82], kurtosis [83], and nonlinear features such as entropy [85], Hjorth parameter [81], etc. These temporal features have the advantage of low-computational cost while providing easily interpretable results. The mean value of the EEG signal represents the average amplitude of the signal and higher mean values may indicate higher overall brain activity, which provides information about the baseline activity level and the overall signal amplitude. The variance measures the fluctuation of the EEG signal around the mean, which reflects the changes in brain activity. The standard deviation is the square root of the variance and is also used to measure the variability of the EEG signal. Skewness measures the asymmetry of the distribution of EEG signals and characterizes possible abnormalities in brain functions. Kurtosis characterizes the spikes and flatness of the EEG signal and indicates the presence of abnormal values or the potential of brain activity.

Hjorth parameters [84] are a group of single-channel features consisting of activity, mobility, and complexity, that provide information about the regularity and complexity of the EEG signal. The activity is calculated based on the variance of amplitude in the EEG signal  $x(t)$ :

$$\text{Activity} = \text{var}(x(t)) = \frac{\sum_{n=0}^{N-1} (x(n) - \bar{x}(t))^2}{N} \quad (9)$$

$$\bar{x}(t) = \frac{1}{N} \sum_{n=0}^{N-1} x(n) \quad (10)$$

where  $\bar{x}(t)$  is the mean of  $x(t)$ .

Mobility measures the mean frequency of the EEG signal:

$$\text{Mobility} = \sqrt{\text{Activity}(x'(t)) / \text{Activity}(x(t))} \quad (11)$$

Complexity evaluates the similarity of the EEG signal to a sinusoidal wave and describes the variability of the EEG signal:

$$\text{Complexity} = \text{Mobility}(x'(t)) / \text{Mobility}(x(t)) \quad (12)$$

Entropy [85] is used to measure the regularity and complexity of the

EEG temporal sequence. A high entropy indicates a high complexity or randomness of the EEG signal, otherwise it indicates a more regular and predictable signal. Kang et al. [107] used four entropy methods to characterize EEG signals, including approximate entropy, sample entropy, permutation entropy. The results showed that the combination of these entropies could better describe the chaotic and non-stationary nature of EEG data. Chao et al. [86] calculated six time-domain features of EEG, including mean, the mean of absolute values of first and second difference, variance, standard deviation, and approximate entropy, and then constructed a 3D feature matrix based on the arrangement of brain electrodes. Heunis et al. [88] constructed a recurrence graph on the raw EEG signal, and then extracted three nonlinear features of recurrence rate, certainty and average diagonal length according to the recurrence quantification analysis. The findings suggested that the nonlinear features based on recurrence quantification analysis can effectively characterize the heterogeneity of ASD.

#### B. Dual-channel Features

Dual-channel features are extracted simultaneously from two channels of the EEG data, which are able to assess the interdependence and interactions between two specific brain regions or electrodes. Frequently used dual-channel EEG features for ASD identification include correlation [91] and cross-correlation [96]. Correlation measures the linear relationship between two EEG signals at each time point and reflects the degree of similarity or coupling between the signals. A common measure of correlation is the calculation of the Pearson's coefficient of correlation (PCC) [97], which is described by Eq. (13). The value of PCC is between  $-1$  and  $+1$ , where  $+1$  implies 100 % positive correlation,  $0$  does not indicate correlation, and  $-1$  implies 100 % negative correlation. Peña et al. [98] calculated the PCC between two channels and converted the 19-channel EEG signal into a  $19 \times 19$  correlation matrix. The matrix was later plotted as a color image using the seaborn heatmap library from Python. Finally, the image information was captured by ResNet [165] and used for ASD identification of the EEG data.

$$P_{xy} = \frac{\text{cov}(xy)}{\sqrt{\sigma(x)\sigma(y)}} \quad (13)$$

where  $\text{cov}(\bullet)$  is the covariance,  $\sigma(x)$  and  $\sigma(y)$  are the standard deviation of  $x$  and  $y$ , respectively.

The cross-correlation calculates the similarity of two EEG signals at different time lags, which represent the time-delay relationship between the signals. The cross-correlation for time series  $x_i$  and  $x_i$  of signals  $x$  and  $y$ , respectively, is defined as follows

$$C_{xy}(\tau) = \frac{1}{N-\tau} \sum_{i=1}^{N-\tau} \left( \frac{x_i - \bar{x}}{\sigma_x} \right) \left( \frac{y_{i+\tau} - \bar{y}}{\sigma_y} \right) \quad (14)$$

where  $\bar{x}$  and  $\bar{y}$  denote the mean,  $\sigma_x$  and  $\sigma_y$  the variance, and  $\tau$  is the time lag.

Ibrahim et al. [123] used cross-correlation functions to quantify the synchronization between EEG channels. They divided the EEG channels into three brain regions, i.e., frontal, central, and posterior. Then, the average EEG synchronization within and between all brain regions was calculated. For a 16-channel EEG segment, a connection matrix of  $16 \times 6$  was obtained. Finally, tri-classification of normal subjects, epilepsy and ASD was achieved using linear discriminant analysis, artificial neural networks, KNN, and SVM.

#### C. Multi-channel Features

Multi-channel features are extracted from multiple channels of EEG simultaneously, and can reveal the potential topology of the brain. Common methods for extracting multi-channel features include network analysis of brain functional connectivity (FC) and microstate analysis.

The FC of EEG [90] can be analyzed in both time and frequency domains. In the time domain, the FC measures the temporal relationship between different brain regions to reveal the dynamic interactions between brain regions. The FC is typically quantified using graph-theoretical analysis [99], which maps EEG signals into complex networks. The key step in the method is the construction of the visibility graph of EEG signals, where each node denotes a data sample in the time series, and an edge connecting two nodes is defined in Eq. (15). Then, basic network metrics including the modularity, average degree, and clustering coefficient are calculated to obtain the FC between brain regions.

$$x(t_2) < x(t_3) + (x(t_3) - x(t_1))t_1 \quad (15)$$

where  $x(t_i) = [x(t_1), x(t_2), \dots, x(t_n)]$  is the EEG time series.

Considering that only a few nodes are strongly or weakly connected in the brain FC networks, Wadhra et al. [100] computed the weighted hierarchical complexity (WHC) for measuring the hierarchical complexity of the topology in the brain network. Firstly, the VG algorithm maps the EEG signals to a network. Then, the weight of each visible edge is computed based on the angle between those visible edges. Finally, the degree of nodes and brain hierarchical complexity are calculated based on the weights. Compared to the other weighted metrics, the WHC is capable of modeling brain topology at different connectivity levels, where dense nodes reveal higher hierarchies and sparse nodes indicate lower hierarchies. The interpretable SVM is used to identify ASD.

The EEG microstate analysis [101] is a multi-channel EEG analysis method based on functional microstates, which considers the entire topographic map of EEG. It can characterize the spatial and temporal characteristics of cortical activity across the entire brain with high temporal resolution [101]. As shown in Fig. 4, the goal of microstate analysis is to extract a set of microstate prototypes from the EEG data and represent the spatiotemporal features [106] of EEG based on the set of microstate prototypes. The microstate analysis can be summarized into four steps. Firstly, all EEG segments in the dataset are aggregated to generate the template data. Secondly, an optimal set of microstate prototypes is evaluated on the template data. Thirdly, the EEG signals are backfitted using this set of microstate prototypes to convert the sample EEG segments into microstate streams. Finally, microstate features are computed based on the microstate streams.

In order to explore the significance of EEG microstates, Milz et al. [102] analyzed four microstate prototypes as class A, class B, class C and class D, and compared the microstate parameters between three task states and the resting state. The results indicated that interplay between these four EEG microstates is necessary for forming visual and verbal thoughts. Moreover, class A is related with vision, microstate B is

associated with language, and class D reflects the degree of individual interoceptive processing particular to the resting state, and Compared to TD children, existing studies have shown that certain temporal features and transition probabilities of the microstates in ASD children are abnormal [103]. D' Croz-Baron et al. [104] found that certain microstates displayed statistically significant differences between ASD children with TD children. Kong et al. [105] evaluated five microstate prototypes through EEG microstate analysis and then generated microstate streams by back-fitting the EEG signals based on these microstate prototypes. Then, features including global field power, global explained variance, mean duration, time coverage and frequency of occurrence were extracted from the microstate streams. Finally, ASD was successfully identified using SVM, confirming that microstate features are effective biomarkers for the diagnosis of ASD.

### 3.2.2. Frequency-domain features

In fact, EEG signals contain multiple frequency bands that are important for ASD identification, such as delta (0.5–4 Hz), theta (4–8 Hz), alpha (8–13 Hz), beta (13–30 Hz) and gamma (30–50 Hz) rhythms, and the oscillations in different frequency rhythms in EEG have specific meanings [114]. Among them, the delta brain wave is the slowest and with the largest amplitude, which usually occurs during the sleep phase; the theta waves occurs during meditation and drowsiness, but not during the deep sleep; the alpha wave is the dominant rhythm when people are awake, quiet or have their eyes closed; the presence of the beta wave usually indicates that people are in a state of concentration, logical thinking, or anxiety; the gamma rhythm is considered to be related to cognitive processing, which usually presents when people are in a state of arousal. However, Time domain EEG features ignore the relationship between different frequency bands in the signal, while frequency-domain features can provide insight into the spectral features associated with different brain states and activities, and are effective in capturing specific frequency information embedded in the EEG data. To obtain the frequency-domain features, the original EEG recordings are first converted into different frequency bands using a frequency domain transform method such as fast Fourier transform [108]. Then, the frequency-domain features, such as power distribution of frequency bands and connections between brain regions, are extracted by power spectral density [111] estimation and brain functional connectivity [90] analysis.

#### A. Fast Fourier Transform

The fast Fourier transform (FFT) [108] is one of the most popular methods for time-frequency transformation. It decomposes the time domain signal into a series of sinusoidal components of different frequencies with different amplitude and phase, which describe the energy distribution and relative time shift of the signal in the frequency domain.

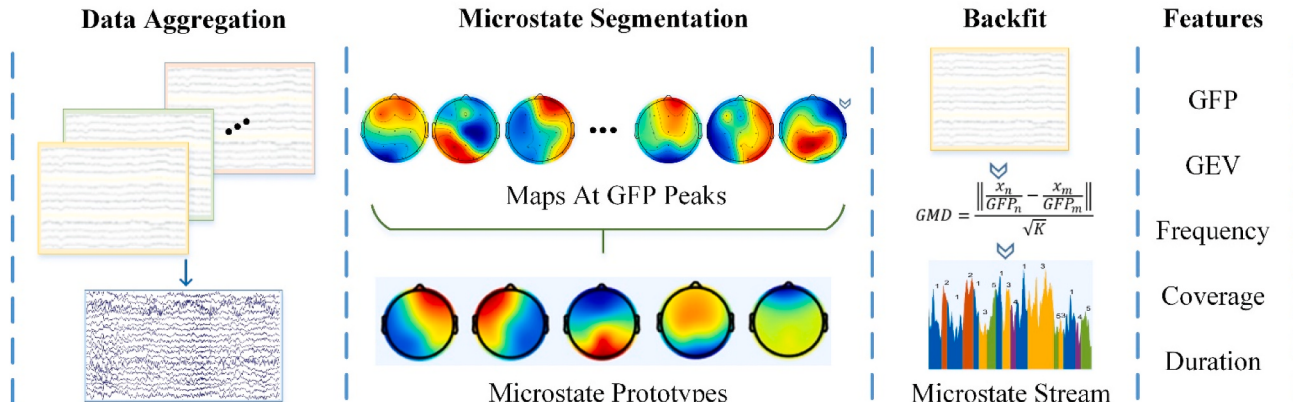


**Fig. 4.** EEG microstate analysis. GFP: global field power, GMD: global map dissimilarity, GEV: global explained variance [95].

Neuhaus et al. [109] analyzed the power distribution of EEG signals at different frequencies using FFT. The absolute power in the bands of delta, theta, alpha, beta and gamma was calculated, and a reduction in the power of the alpha band for ASD children was detected. Wang et al. [110] performed FFT on the EEG signals, calculated the power of four frequency bands of Fz, Pz, Oz, and Cz electrodes and their average values from the EEG signals. After statistical analysis, it was found that the delta band power values at the Fz electrode were significantly increased in ASD children compared to TD. However, the FFT uses periodic sinusoidal waves to represent the original signals, leading to limitations in analyzing non-periodic signals such as EEG signals.

### B. Power Spectral Density Estimation

The power spectral density (PSD) estimation [111] is to transform the EEG signal whose amplitude varies with time into an EEG power spectral that varies with frequency. The PSD of EEG can fundamentally reflect the distribution of the power energy of frequency components in the EEG data, and quantify relative contribution of each frequency for the overall signal, thus useful information such as periodicity and spectral peaks hidden in the signal can be discovered. Typically, PSD estimation starts by splitting the raw signal into shorter smoother segments, which ensures that the signal's statistical properties keep approximately constant over the duration of each segment. Then, each signal segment is characterized as a set of frequency components obtained by FFT. Finally, the power spectrum is obtained by calculating the power at each frequency, and then is normalized to obtain the PSD. Ranjani et al. [112] adopted PSD estimation to characterize the multi-channel EEG signal in the frequency domain, and converted the frequency-domain representation into a 2D image called PSD energy diagram (PSDED). Firstly, the 16-channel EEG signal is decomposed into 32 frequency bands, and then PSDED is constructed by calculating PSDs based on different frequency bands. After that, a deep convolutional neural network is applied to automatically extracting features from PSDED and a fully-connected layer is finally utilized to classify the signals into autistic, epilepsy and normal. Esqueda-Elizondo et al. [89] measured the attention of ASD children by PSD estimation in Theta, Alpha and Beta bands. For each channel, the relative power of Theta, Alpha and Beta, Theta-Beta ratio, Theta-Alpha ratio, and Theta-(Alpha + Beta) ratio is computed. The states of "Attention" and "No Attention" in ASD children are classified using a multi-layer perceptron neural network. The results demonstrated that these PSD characteristics were shown to be associated with attention and neurofeedback in children with autism. However, the accuracy and reliability of PSD estimation is limited by the EEG signals with short dataion since it requires the segmentation of EEG signals by non-overlapping windows.

### C. Functional Connectivity Analysis

In the frequency domain, the functional connectivity (FC) [90] of EEG reflects the relationship between different frequency components of the EEG signal. The first step of FC analysis is the same as in PSD estimation, where the original EEG signal is decomposed into different frequency components such as delta, theta, alpha, beta and gamma bands using frequency domain analysis such as FFT. Then, the strength of the FC between the EEG signals in each band is evaluated by calculating phase-locked value (PLV) [93] and coherence [92]. Among others, the PLV quantifies the phase synchronization between two channels representing the degree of FC or synchronization between brain regions. A higher PLV indicates stronger phase coupling and potential communication between brain regions [94]. To obtain PLV, the information in the transient phase is first extracted from the EEG signal by Hilbert transform or wavelet transform, after which the phase difference between the EEG signals of different channels is calculated. Coherence is a widely used measure of FC that represents the correlation between different brain regions by capturing the phase and amplitude

relationships in different frequency bands [95]. Firstly, the power distribution over different frequency bands is calculated by Fourier transform. Then, the coherence is obtained by calculating the crossover spectrum between different channels. Kang et al. [107] calculated the coherence between EEG channels using phase lag index separately, including Fz-Fp2, O1-Fp1, P3-F3, T7-F3, Fz-F4, and O2-Fz. In addition to the correlation-based FC, both entropy and PSD are extracted and then the feature group with the maximum relevance to the class label and the minimum redundancy among features is selected. Finally, accurate ASD identification is achieved by a linear SVM classifier. Alotaibi et al. [113] quantitatively characterized FC networks by calculating graph-theoretic parameters based on PLV and identified children with ASD using a cubic SVM. The results discovered substantial changes in brain functional connectivity in the theta band in ASD children.

#### 3.2.3. Time-frequency features

Time-domain features provide temporal information of the EEG recordings, while ignoring variations in specific frequencies. Frequency-domain features effectively characterize EEG spectral properties, but may not perceive the temporal changes and dynamics in the signals. By contrast, features in time-frequency domain provide both temporal and spectral information of the EEG data [114]. The feature extraction methods involve short-time Fourier transform (STFT), wavelet transform (WT) and empirical mode decomposition (EMD) [115], which are capable of detecting transient frequency changes, event-related potentials, and dynamic brain activity.

#### A. Short-time Fourier Transform

Short-time Fourier transform (STFT) [116] assumes that the signal is stationary in the short time [117]. Through moving the windows along the time axis, the Fourier transform of the time period in each window is calculated and time-varying spectrum is obtained. Firstly, the EEG signal is divided into consecutive and overlapping segments with fixed window size and step size. The window size determines the time-frequency resolution of STFT, i.e., it is proportional to frequency resolution and is inversely proportional to the time resolution. A step size is used to determine the amount of overlap between windows. The step size of 50 % of the window size is typically selected to achieve a continuous and smooth representation. Next, a window function such as the Hamming window [118] is used to multiply the EEG segments sequentially along the time axis in order to minimize the spectral leakage in FFT. After that, the spectra of all EEG segments are obtained by FFT to generate time-frequency representations. Tawhid et al. [119] used STFT to generate a time-frequency spectrogram image of the EEG data. The frequency bands in the spectrogram change over time, and each color in the image reflects different energy values in the EEG data. Then, texture features of the images were extracted, and important features were selected by principal component analysis and fed to a SVM classifier for ASD classification. The STFT is the simplest method in time-frequency analysis. However, the time-frequency resolution in STFT is fixed, which limits its ability to accurately capture fine-scale variations of EEG signals.

#### B. Wavelet Transform

The wavelet transform (WT) [120] constructs independent frequency band components using a series of wavelets generated by a specific wavelet function (mother wavelet) with different scales of dilation and translation. The WT provides variable time-frequency resolution with efficient time-frequency localization to capture transient brain states more accurately.

A three-level WT is given in Fig. 5. The WT filters the signal level by level through a multi-resolution decomposition algorithm, i.e., high-pass and low-pass filters set at each WT level, and the filter coefficients are generated by dilation and translation [121]. The low-pass

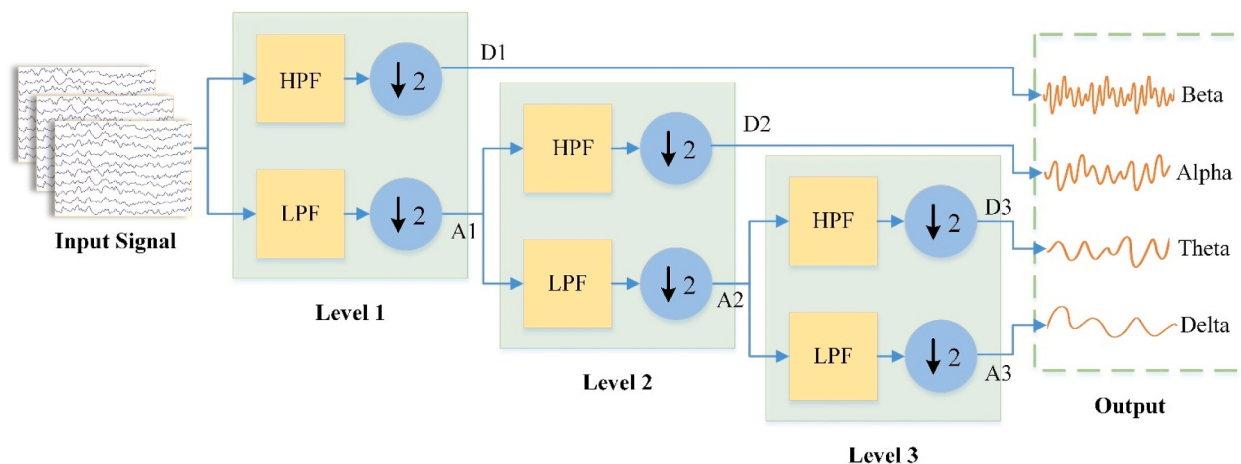


**Fig. 5.** A three-level wavelet transform. HPF: High-pass filter, LPF: Low-pass filter.

filter, which acts as a smoothing filter, is designed to capture the low-frequency components of the EEG signal, obtaining approximate coefficients that represent the overall trend and slower variations of the EEG. The high-pass filter acts as a high-frequency enhancement filter. It extracts high-frequency information from the EEG signal, including sharp changes and fine details. The high-pass filter outputs detail coefficients that represent fine variations of the EEG. By iteratively applying low-pass and high-pass filters to the EEG signal and down-sampling the resulted coefficients, the WT decomposes the original EEG signal into multi-level detail coefficients (D1, D2, D3) and approximation coefficient (A3), with each level representing a different frequency band.

In addition to computing the mutual correlation and measuring the synchronization between EEG channels, Ibrahim et al. [123] also adopted WT to decompose the EEG data into five frequency bands including delta, theta, alpha, beta, and gamma. Specifically, they decompose EEG fragment into a series of detail coefficients (D1-D6) and approximation coefficients (A1-A6) using a six-level DWT decomposition and Daubechies-four mother wavelet, after which the coefficients of D3, D4, D5, D6 and A6 are retained to represent the five subbands of the EEG signal. Then, standard deviation, Shannon entropy, band power and largest Lyapunov exponent [124] were computed from these subbands. These features are fed into linear discriminant analysis, artificial neural networks, KNN, SVM for classification. This approach has been successful in a triple classification task, i.e., normal vs. epilepsy vs. autism. Alturki et al. [125] decomposed the EEG signal into five bands by four-level DWT using Daubechies-four as the mother wavelet function, and then extracted features from the five bands, including log band power, variance, standard deviation, kurtosis, and Shannon entropy. Finally, the identification of normal subjects, epileptic patients and ASD patients was achieved using linear discriminant analysis, artificial neural networks, KNN, and SVM.

### C. Empirical Mode Decomposition

Empirical mode decomposition (EMD) [67] is a data-driven adaptive nonparametric approach [134] that decomposes a signal into a set of intrinsic mode functions (IMFs) [130], which are narrowband oscillatory components determined from the dynamic properties of the raw signal [131], providing a local time-frequency representation of the signal. The IMFs have to satisfy two conditions [132]:

- 1) The difference between the number of extrema and the number of zero crossings must either be zero or one.
- 2) The mean value of the local maxima envelope and the local minima envelope must be zero.

To apply EMD to the EEG signal, firstly, all local maxima and minima in the EEG signal  $x(t)$  are identified and connected to construct the upper envelope and the lower envelope, respectively, and their mean values are calculated to obtain the mean envelope  $m(t)$ .

Next, the signal  $h_1(t)$  is obtained by subtracting the mean envelope from the EEG signal  $x(t)$ . If  $h_1(t)$  fulfills the two conditions mentioned above, it is considered as the first IMF  $c_1(t)$ . Otherwise, the above steps are repeated  $i - 1$  times until  $h_i(t)$  fulfills the conditions. Then,  $h_i(t)$  is considered as the first IMF  $c_1(t)$ .

$$h_1(t) = x(t) - m(t) \quad (16)$$

$$c_1(t) = h_i(t) \quad (17)$$

The new time series  $\tilde{x}(t)$  is obtained by subtracting the first IMF  $c_1(t)$  from  $x(t)$ :

$$\tilde{x}(t) = x(t) - c_1(t) \quad (18)$$

The subsequent IMFs and new residual signals  $r_n$  are obtained by performing the above steps iteratively until  $r_n$  becomes monotonous and cannot be further decomposed. The  $x(t)$  can be represented as in Ref. [133]:

$$x(t) = \sum_{i=1}^n c_i(t) + r_n \quad (19)$$

Since EMD does not rely on predefined basis functions, such as sinusoidal functions or specific wavelet functions, it adaptively decomposes IMFs directly from the data, making it more appropriate for analyzing non-stationary EEG signals. Hadoush et al. [135] used EMD to extract IMFs features, analyze the differences between children with mild and severe ASD, and judge ASD severity based on the measured differences. They created the second-order difference plot (SODP) [136] from IMFs, and calculated the ellipse area [137] and central tendency measure (CTM) [138] of the SODP. This study found that children with severe ASD exhibited less oscillations of IMF features, less CTM values, more stochastic SODP plots and higher elliptical area values.

### 3.3. Classification

Automatic autism identification based on traditional machine learning starts with data preprocessing and feature extraction, after which a suitable classifier is selected to analyze and categorize the extracted features. For a classification task, the dataset is split into two subsets, i.e. the training set and the test set. A classifier is constructed based on the training set, then evaluated on the test set. This section summarizes classical classifiers that are often used in ASD identification.

#### A. Support Vector Machine

Support vector machine (SVM) [140] is a powerful supervised machine learning algorithm. Initially, SVM was developed as a binary classifier capable of classifying linearly separable data. As shown in Fig. 6a, the SVM aims to create a hyperplane that best discriminates between positive and negative samples. It maximizes the margin between the separating hyperplane and the data [141], which enables the SVM to solve binary classification problems efficiently. However, real-world data are not always linearly separable, where kernel methods are required to transform the lower-dimensional input data into a higher-dimensional feature space, thus making the data linearly separable, as shown in Fig. 6b. Popular kernels include Gaussian kernel, polynomial kernel, radial basis function (RBF) kernel and sigmoid kernel. Since SVM has powerful classification abilities, it has been adopted in various research fields, e.g., image classification, text analysis, and bioinformatics. About 50 % of the studies in traditional machine learning for EEG-based ASD recognition have used SVM as the classifier. Abdolzadegan et al. [127] extracted the linear and nonlinear features of EEG signals and then used SVM and KNN classifiers for final decision making. In the experiment, the classification accuracy of SVM is 90.57 %, which is better than using the KNN approach.

#### B. Random Forest

Random forest (RF) [142] is a typical ensemble learning algorithm that makes accurate and robust predictions by combining the strengths of multiple weak classifiers. As shown in Fig. 7 it starts by aggregating different decisions by creating a large number of decision trees, which are generated from N training subsets randomly selected from the original dataset. Each decision tree is trained independently on a subset of the data, which reduces the risk of overfitting and enhances the generalization ability of the model. When the RF model receives a new input sample, each decision tree in the forest evaluates the sample independently and predicts the category labels. Then, the final prediction for the input sample is obtained based on the majority voting mechanism, i.e., the category label with the most votes among all decision trees will be assigned to the input sample. The RF is characterized by the diversity of their decision trees, but there is no connection or collaboration between these decision trees since each decision tree operates independently based on its corresponding subset of data. Grossi et al. [144] extracted multi-scale ranked organizing maps to characterize EEG signals, followed by ASD identification using multiple classifiers, such as RF, KNN and K-Contractive Map. The best result was achieved with 92.8 % accuracy using a random forest approach.

#### C. Multilayer Perceptron

Multilayer Perceptron (MLP) [145] is a feedforward artificial neural network that includes an input layer, multiple hidden layers and an output layer. The parameters in MLP include weights, biases, and activation

functions, which collectively shape the network architecture, define its learning capabilities, and enable it to capture complex nonlinear relationships. There is a weight between each pair of neurons in neighboring layers that determines the importance of a particular input feature or neuron to the network output. During the training stage, the network learns to adjust these weights iteratively to minimize the prediction error and improve the accuracy. The bias introduces a tunable constant value between the neuron's input and the activation function, which is added to the weighted sum of the neuron's inputs, and the result is then passed to the activation function. Thus, it affects the activation threshold of the neuron, increasing the flexibility of the neural network and allowing it to better adapt to different input data. The activation functions are nonlinear functions that map the inputs of neurons nonlinearly and control the outputs of each neuron, enabling MLP to model complex nonlinear relationships. Common activation functions include Sigmoid, ReLU, and Tanh, which are defined in Eq. 20–22:

$$\text{sig}(x) = \frac{1}{1 + e^{-x}} \quad (20)$$

$$\text{relu}(x) = \begin{cases} 0, & x \leq 0 \\ x, & x > 0 \end{cases} \quad (21)$$

$$\tanh(x) = \frac{e^x - e^{-x}}{e^x + e^{-x}} \quad (22)$$

MLP is highly flexible and can be adapted to various tasks by adjusting the architecture, e.g., the number of layers, the number of neurons, and activation functions. Cheong et al. [128] used DWT to decompose EEG data into frequency components and extracted statistical features of components, and finally trained the MLP to categorize the signals into three autism severity classes, i.e., mild, moderate and severe. Fig. 8 shows a neural network having 9 input neurons, 8 hidden neurons, and 3 output neurons. The experimental results showed a high classification accuracy of 92.3 %.

#### D. K-nearest Neighbors

K-nearest neighbors (KNN) [146] is a nonparametric approach, which makes predictions or classifications by the similarity between samples. Different from other supervised learning algorithms, KNN considers information from multiple neighbors rather than relying solely on a single sample, thus reducing the impact caused by outliers. As shown in Fig. 9, when classifying or regressing a sample, the distance between that sample and other training samples is first calculated. Commonly used distance metrics include Euclidean distance, Manhattan distance, and cosine similarity. Second, following the idea that similar samples are close to each other in the feature space, KNN selects K training samples closest to that sample based on the distance. Finally, prediction is performed according to the information of K neighbors, and

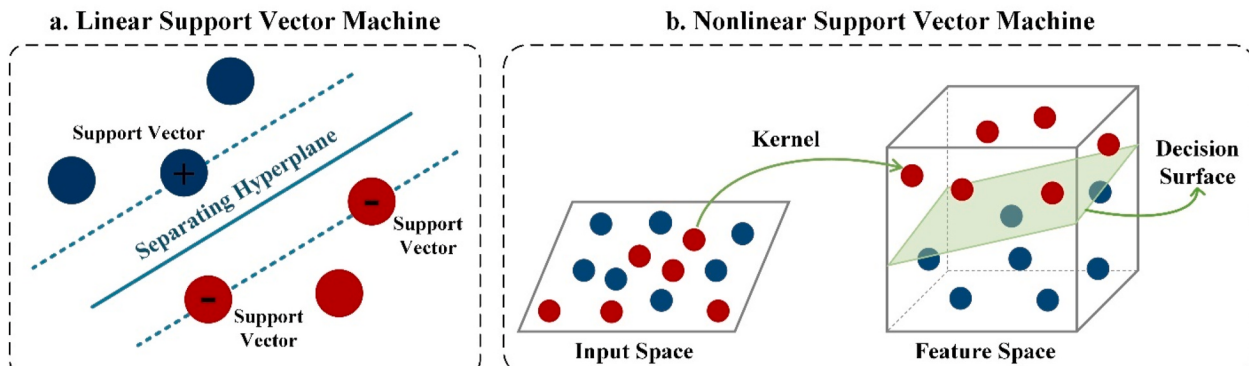


Fig. 6. Support vector machine.

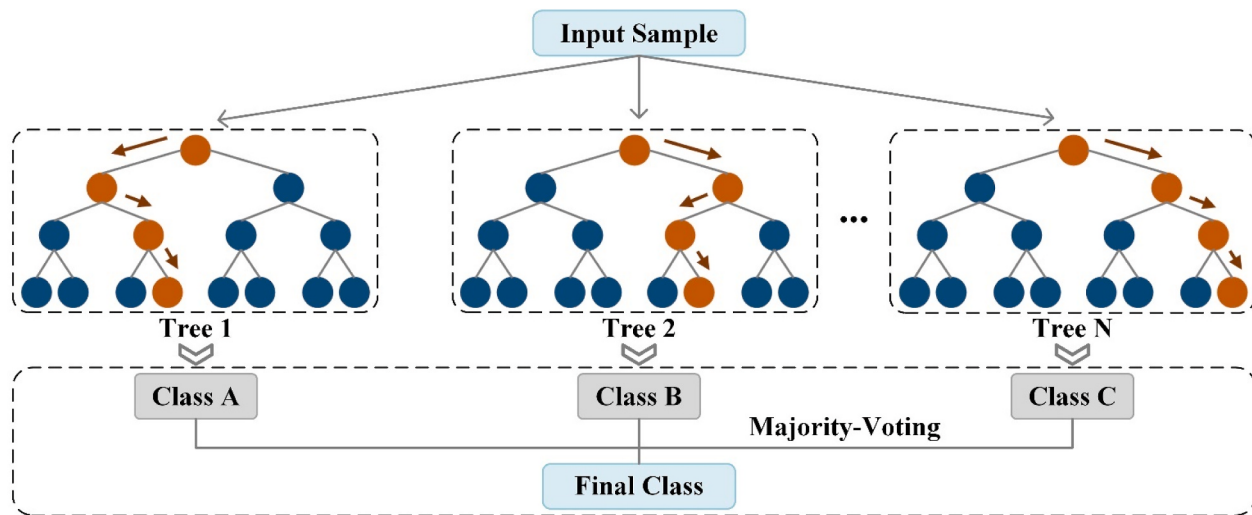


Fig. 7. Random forest.

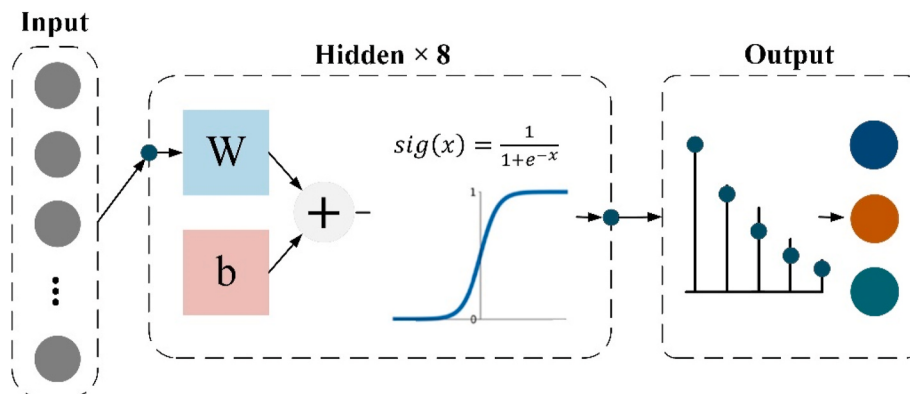


Fig. 8. Multilayer perceptron.

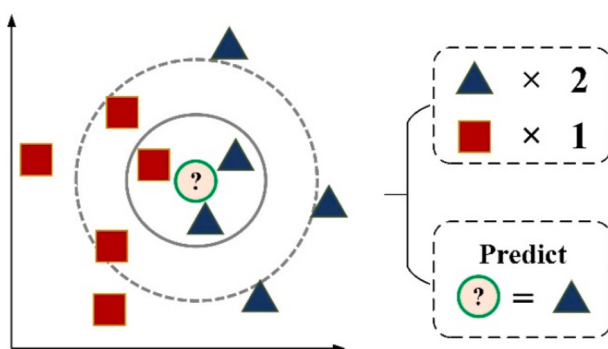


Fig. 9. K-nearest neighbors.

the new sample is assigned to the category with the largest proportion of the K nearest neighbors. The KNN does not require assumptions about the underlying feature space [147] and can be applicable to various data types. Therefore, it is widely used in image classification, text analysis and biological sequence analysis. Ibrahim et al. [123] extracted five features of EEG, including standard deviation, cross-correlation, band power, Shannon entropy and largest Lyapunov exponent, respectively. After that, triple classification of normal, epileptic and ASD was achieved using linear discriminant analysis, artificial neural network, KNN and SVM. The experimental results showed that triple classification using Shannon entropy features and KNN achieved the highest accuracy

of 94.62 %.

#### E. Logistic Regression

In machine learning, logistic regression [148] is a popular algorithm for solving binary classification problems. As shown in Fig. 10, its primary goal is to build a probabilistic model. The feature weight and bias of the sample are calculated through linear regression, and then the result of the linear combination is mapped to a probability value between 0 and 1 through a logistic function, such as the Sigmoid function. By setting a threshold, output values above the threshold are categorized into one class and those below the threshold are categorized into the other class. Compared to other complex classification algorithms, logistic regression has a relatively fast training and prediction process that

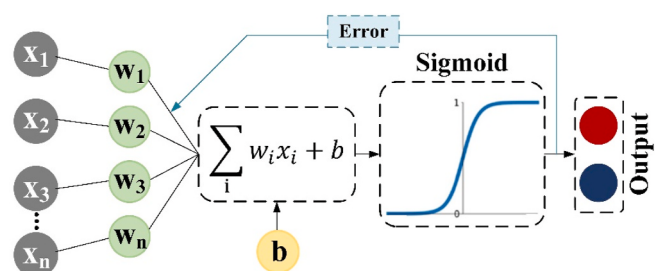


Fig. 10. Logistic regression.

does not require very large amounts of computation. In addition, it has better model interpretability, which can help understand the influence of different features on the classification results. Thapaliya et al. [87] performed preprocessing and feature extraction of EEG signals and eye movement data, and then simply integrate the features. After that, classification with multiple feature combinations were conducted using SVM, LR, DNN and Naive Bayes, respectively. The experimental results showed that LR performs best in the ASD recognition task with an accuracy of 100 %.

### 3.4. Summary

We summarize the traditional machine learning methods for EEG-based ASD identification in Table 3, which illustrates the EEG datasets, data pre-processing methods, feature extraction methods, classifiers, and identification performance of ASD for each method.

## 4. Deep learning

The expansion of data scale and the rapid development of computer hardware provide excellent training resources for deep learning. Therefore, deep learning-based autism identification are becoming increasingly popular. Instead of performing feature extraction, feature selection, and classification, separately, deep learning automatically discovers distributed feature representation of EEG data by combining lower level features to form more abstract, higher level features that represent attribute categories [152]. We divide the deep learning methods in EEG signal-based autism identification according to the underlying models, including the convolutional neural network, recurrent neural network, and graph convolution network.

### 4.1. Convolutional neural network-based methods

Convolutional neural network (CNN) [153] is an extension of MLP that extracts features from the input data through convolutional operations. The different is that the connections of CNN neurons are not fully-connected, where each neuron is only connected to a localized region (i.e., the receptive field) in the previous layer. This local connectivity models the way as our brain perceives and processes information hierarchically, allowing the CNN to effectively capture local salient information. At the same time, weights of connections are shared between certain neurons in the same layer in a CNN, which enables the network to learn and capture specific features. This not only reduces the number of model parameters, but also improves the model generalization ability [154]. The capabilities of robust feature extraction and spatial relationship modeling of CNN make it become one of the most important network models in deep learning. In EEG-based ASD identification, CNN is also a mainstream method and has been demonstrated with excellent feature extraction and classification performance.

The traditional CNN is usually composed of the convolutional layer, the pooling layer, and the fully connected layer. The performance of CNN can be adjusted by changing the number of layers, the order, as well as the size and number of kernels. Tawhid et al. [155] used traditional machine learning and deep learning models for ASD identification of EEG signals. Firstly, the preprocessed signal was transformed into a 2D spectrogram image using short-time Fourier transform. The spectrogram image was sent to traditional machine learning and deep learning models, respectively, to achieve deep feature extraction and classification. For traditional machine learning-based models, texture features were extracted and classified using six different classifiers. For deep learning-based models, three different CNN models were tested separately, as shown in Fig. 11. These models were validated on a dataset from King Abdulaziz University (KAU) Hospital, Saudi Arabia, Jeddah [53]. The dataset consisted of 9 normal children and 11 ASD children, and the EEG signals were collected on 16 channels at a sampling rate of 256 Hz. The results showed that the deep learning model

achieves higher accuracy on the EEG dataset. Ari et al. [156] also applied CNN models for the identification of ASD based on EEG recordings. The framework of the study is shown in Fig. 12.. First, the Douglas-peucker algorithm was used to reduce the number of samples without compromising the EEG structure for each channel. Then, EEG rhythms were extracted using wavelet transform, which are sparsely encoded using a matching pursuit algorithm and converted into images. To improve the efficiency of CNN, a data augmentation method was applied based on extreme learning machine autoencoder to increase the number of training samples. Finally, EEG signals of ASD and healthy children were classified using a pretrained ResNet [163]. The framework was validated on a dataset from KAU Hospital, Saudi Arabia, Jeddah [53]. Experimental results showed that the CNN-based method can effectively extract salient features from EEG signals, resulting in high classification performance. In addition, transfer learning is widely used in EEG-based ASD diagnosis. Din et al. [157] and Stamate et al. [158] used features generated by pre-trained CNN models for ASD identification, including GoogLeNet [159], AlexNet [160], MobileNet [161], SqueezeNet [162] and ResNet, etc. The results showed that the pre-trained CNN model can improve the accuracy and efficiency of ASD identification. However, the traditional CNN is difficult to comprehensively capture the features of EEG signals from the temporal and spatial dimensions, which affects the classification accuracy using EEG. Moreover, a specific network model is only applicable to one experimental paradigm or task and not generalized for multiple tasks.

To achieve automatic identification of autism, Wadhra et al. [167] and Tan et al. [164] used EEGNet [165], a general-purpose network for EEG analysis. The EEGNet is a compact CNN developed for EEG-based brain-computer interfaces (BCIs), which has generalizability across paradigms and has been applied to tasks such as motor imagery classification, epilepsy recognition [166], etc. As shown in Fig. 13, the EEGNet is composed of four stages, i.e. 2D convolution, depthwise convolution, separable convolution, and classification. Firstly, the 2D CNN layer extracts local features from the pre-processed EEG data. After that, the local features are fed into the depthwise convolutional layers with a channel-by-channel convolution. The depthwise convolution is different from common convolution that uses different kernels to extract features from multiple channels simultaneously. In contrast, depthwise convolution uses different kernels to extract features from each data channel separately. In EEGNet, the depthwise convolution uses the kernels with the size of  $n \times 1$  to extract spatial features of the EEG signal. Later, these features are fed into a separable convolution, which consists of a depthwise convolution and a pointwise convolution. The depthwise convolution uses the kernels with the size of  $1 \times n$  to learn implicit time-domain information from the input data; while the pointwise convolution is used to optimize the combination of feature maps. Finally, a classifier such as MLP is utilized to classify the obtained EEG features for automatic ASD identification.

Dong et al. [169] found that the mainstream neural network models become insufficient in discriminating EEG in paradigms where the intensive individuality of subjects and non-stationarity of problem development are explicit. Therefore, they proposed a fast reconfigurable CNN driven by reinforcement learning, the architecture of which is shown in Fig. 14. A CNN model with a determined structure and hyperparameters was generated through Q-Learning algorithm, and the CNN model was regarded as a discrete system for optimization. As the input samples change, the Q-Learning algorithm reconstructs the CNN model so that it can adapt to the personalized EEG samples. The ASD dataset used in the study were obtained from the State Key Laboratory of Cognitive Neuroscience and Learning, Beijing Normal University. It consisted of 98 normal children and 86 ASD children, and the EEG signals were collected on 8 channels at a sampling rate of 1000 Hz. Experimental results show that the method can better adapt to scenarios where subject diversity and brain disease development are.

**Table 3**

Traditional machine learning methods for ASD diagnosis using EEG data. ICA: , SVM: Support Vector Machine, KNN: K-nearest Neighbor, NB: Naive Bayesian, EPNN: Enhanced Probabilistic Neural Network, K-CM: K-Contractive Map, LDA: Linear Discriminant Analysis.

Method	Dataset	Pre-processing Techniques	Features	Classifier	Performance Metrics in (%)
Bosl et al. [48] 2011	46 High-risk vs 33 TD; 64 Channels; 250 Hz	Band-pass filter	Modified Multiscale Entropy	SVM; KNN; NB.	Accuracy (SVM) = 70.00 Accuracy (KNN) = 90.00 Accuracy (NB) = 80.00
Ahmadolou et al. [54] 2012	9 ASD vs 9 TD; 19 Channels; 256 Hz	Butterworth Filter	Wavelet Decomposition; Fuzzy Synchronization Likelihood	EPNN	Accuracy = 95.50
Jamal et al. [143] 2014	12 subjects; 128 Channels		Brain Functional Connectivity	Discriminant Analysis; SVM	Accuracy = 94.70  Sensitivity = 85.70 Specificity = 100
Cheong et al. [128] 2015	5 Mild vs 11 Moderate vs 14 Severe;	Bond-pass Filter	Discrete Wavelet Transform;	MLP	Accuracy = 92.30
Grossi et al. [144] 2017	15 ASD vs 10 TD; 20 Channels; 256 Hz	De-artifacting	Multi Scale Ranked Organizing Maps; Multi Scale Entropy	RF KNN K-CM	Accuracy (RF) = 92.86  Accuracy (KNN) = 87.3 Accuracy (K-CM) = 85.71
Djemal et al. [126] 2017	9 ASD vs 10 TD; 16 Channels; 256 Hz	Segmentation; Band-Pass Filter;	Discrete Wavelet Transform; Entropy	ANN	Accuracy = 99.71
Heunis et al. [88] 2018	16 ASD vs 46TD;  17 Channels; 250 Hz	Band-pass filter;  De-artifacting; Down-sampled; Average Reference	Recurrence Quantitative Analysis;  Sample Entropy; Detrended Fluctuation Analysis	SVM MLP LDA	Accuracy = 92.92  Sensitivity = 100 Specificity = 85.70
Bosl et al. [55] 2018	99 ASD vs 89 TD;  19 Channels; 250 Hz	Band-pass Filter;	Recurrence Quantitative Analysis;  Detrended Fluctuation Analysis, Sample Entropy	SVM	Accuracy = 95.00
Kang et al. [107] 2018	52 ASD vs 52 TD; 19 Channels; 1000Hz	FieldTrip; De-artifacting	Power Spectral Density; Bicoherence; Entropy; Coherence	SVM	Accuracy = 91.38
Ibrahim et al. [123] 2018	90ASD vs, 100 Epileptics vs, 200 TD	De-artifacting	Wavelet Transform; Shannon Entropy; Largest Lyapunov Exponent; Standard Deviation; Band Power; Cross-correlation	KNN	Accuracy = 94.60
Jayarathna et al. [149] 2019	8 ASD vs 9 TD; 10 Channels, 250 Hz	High-pass Filter De-artifacting ICA	Functional Connectivity	JRip RF Logistic	Accuracy (JRip) = 98.06 Accuracy (RF) = 98.00 Accuracy (L) = 96.63
Hadoush et al. [135] 2019	18 mild ASD vs 18 severe ASD;  64 Channels; 50 Hz	Band-pass Filter	Empirical Mode Decomposition: Second-order Difference Plot, Ellipse Area, Central Tendency Measure	ANN	Accuracy = 97.20
Tawhid et al. [119] 2021	12 ASD vs 4 TD; 16 Channels, 256 Hz	Band-pass Filter	Short-time Fourier Transform Spectrogram Image	SVM	Accuracy = 95.25 F1 Scores = 96.70
Abou-Abbas et al. [139] 2021	50 High-risk vs 44 TD; 128 Channels; 500 Hz	De-artifacting; ERP Extraction	Empirical Mode Decomposition; IMF Energy; Shannon Entropy; Statistical Features	KNN SVM	High-risk vs. TD: Accuracy (SVM) = 88.44 HR-ASD vs. HR-noASD: Accuracy (KNN) = 74.00
Li et al. [150] 2022	95 ASD vs 91 TD; 64 Channels;  2048 Hz	MNE-python; EEG Source Localization	Spectral Estimation; Long-range Temporal -correlations;	SVM Logistic	Accuracy >80.00
Wadhhera et al. [100] 2023	30 ASD vs 30 TD; 21 Channels 256Hz	Band-pass Filter; Visually Inspected; ICA	Functional Connectivity Weighted Hierarchical Complexity	RF Explainable SVM	Accuracy = 98.76 Sensitivity = 99.87 Specificity = 96.52
Peketi et al. [151] 2023	15 ASD; P300; 8 Channels; 250 Hz	De-artifacting	Variational Mode Decomposition	SVM	Accuracy = 91.12 F1 Scores = 91.18 AUC = 96.60

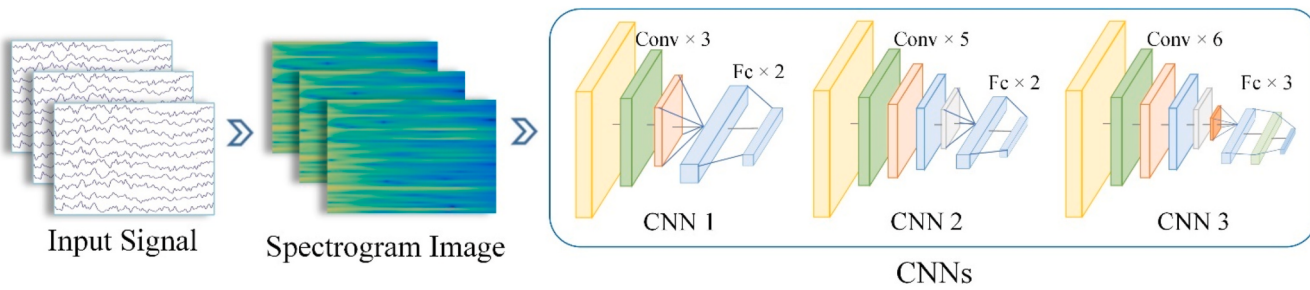


Fig. 11. CNN-based 2D-EEG spectrogram analysis in ASD diagnosis [155].

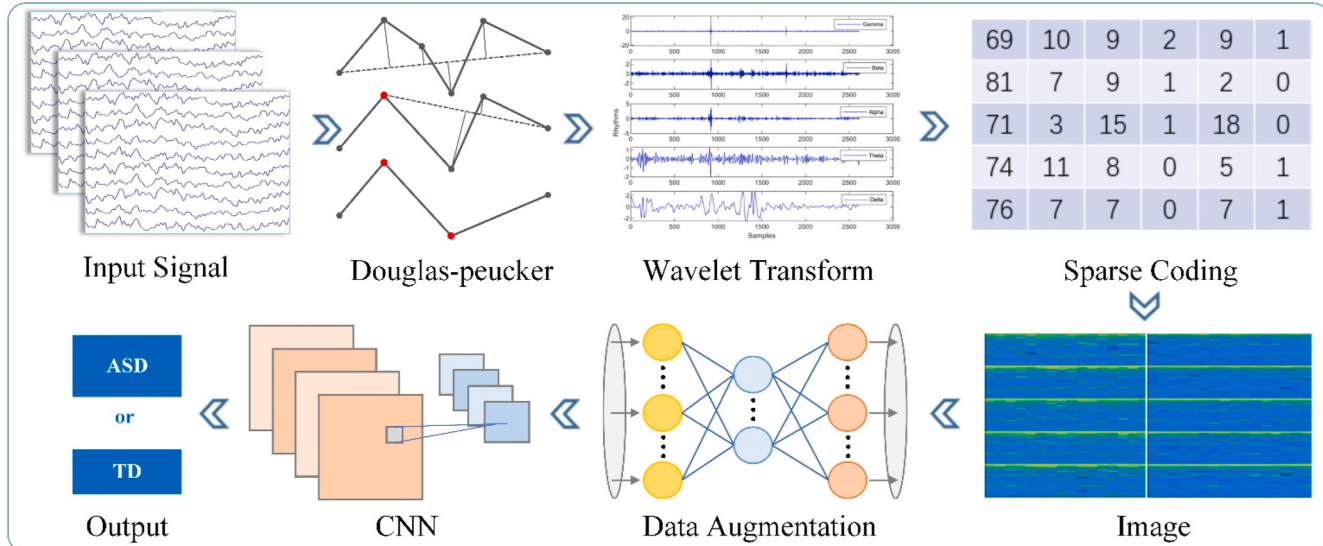


Fig. 12. Detection of autism using Douglas-peucker algorithm, wavelet transform, sparse coding based feature mapping, data augmentation and convolutional neural network techniques using EEG signals [156].

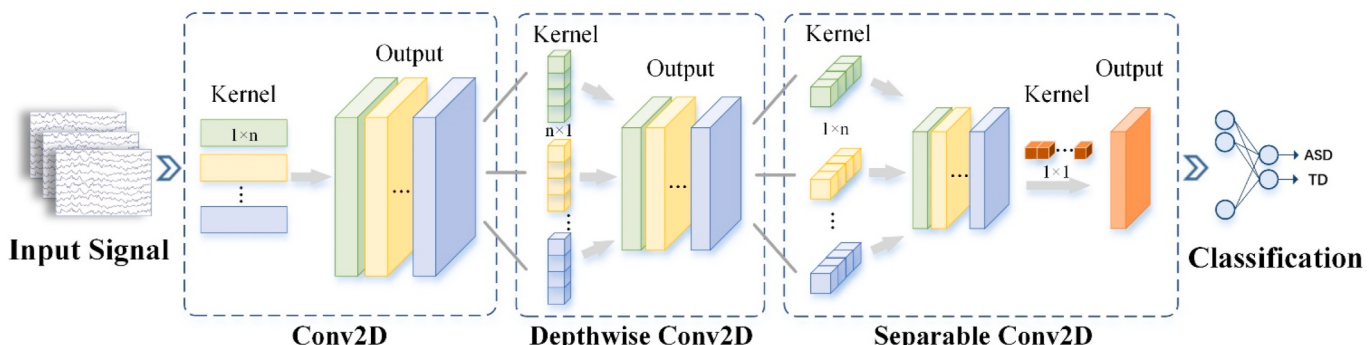


Fig. 13. EEGNet [165].

#### 4.2. Recurrent neural network-based methods

Recurrent neural network (RNN) [170] is a type of neural network that is adapt at handling long-term dependencies, and it is capable of accepting both the current input data and previously received input data. Therefore it is more suitable for sequence modeling tasks. Long short-term memory (LSTM) [73] is a special type of RNN that can learn long-term dependency information from sequence data. A single LSTM block consists of three gates called the input gate, the forget gate and the output gate. The input gate decides whether to use the input sequence to modify the current state on the block. The forget gate is used to keep or remove the prior state on the LSTM block, while the output gate keeps

track of the output information and decides whether to move the current hidden state to the next time step. The LSTM is widely used in the analysis of time series, such as EEG signal.

Ali et al. [171] used a bidirectional long short-term memory (BiLSTM) network to implement EEG-based autism identification. The model structure is shown in Fig. 15. This bidirectional structure combines two LSTM blocks with different propagation directions to classify the EEG data samples. The dataset in this experiment consisted of 39 ASD children and 14 normal children, and the EEG signals were collected on 128 channels at a sampling rate of 500 Hz. The experimental results showed that BiLSTM is more desirable than LSTM to deal with nonlinear and non-stationary problems of ASD identification based

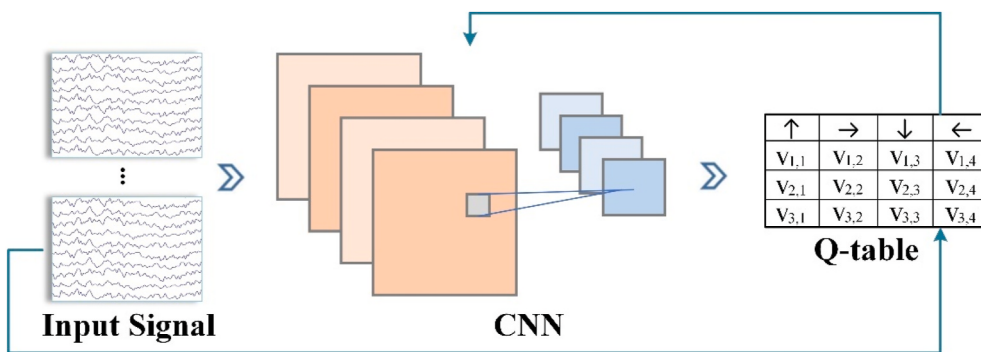


Fig. 14. Fast reconfigurable CNN [169].

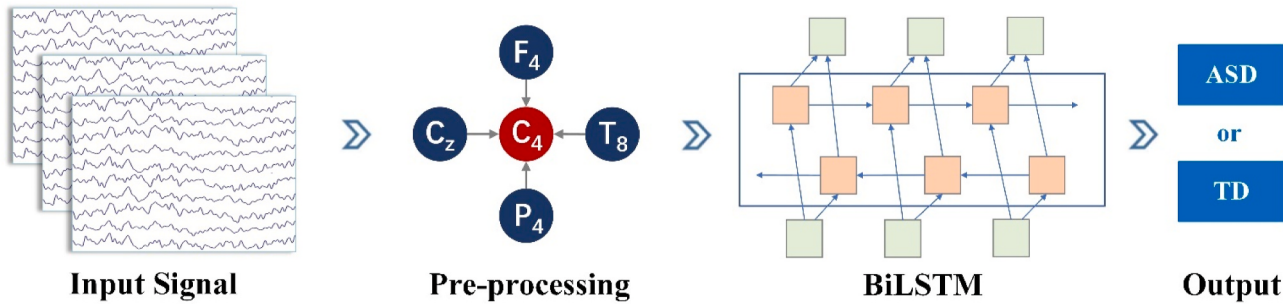


Fig. 15. BiLSTM based ASD identification model [171].

on EEG data. Later, Ali et al. [172] improved the model by combining CNN and BiLSTM, as shown in Fig. 16, the CNN is used to extract the local features of EEG signals, and the BiLSTM is used to capture the temporal dependencies in EEG signals for ASD classification. The experimental results showed that the classification performance combining CNN and BiLSTM is better than that using a single model. This is because CNN is good at extracting local features of EEG signals, and BiLSTM makes up for the temporal dependencies that CNN cannot capture.

#### 4.3. Graph convolution network-based methods

Graph convolutional network (GCN) [168] is a method to describe the internal connections between different graph nodes, and can be used to learn the relationships between multiple channels in EEG signal. The GCN extends the CNN by combining it with graph theory, which is suitable for feature extraction for graph-structured data, e.g., the FC of the brain that measures the correlation between different brain regions. In recent years, the GCN has gradually been applied in brain disease diagnosis based on EEG data. Tang et al. [173] constructed a deep EEG superresolution (Deep-EEGSR) model by applying GCN and dynamic filtering mechanism for EEG analysis. The Deep-EEGSR consists of five

modules in total, as shown in Fig. 17. Firstly, the data of missing channels were roughly estimated by spherical spline interpolation to reconstruct the detailed information of the target EEG. Secondly, the channelwise 2D convolution was used to perform temporal filtering on each channel of the EEG to enhance individual representations of time-series information in each channel. Thirdly, the Gaussian kernel function on the distance between the two electrodes was applied to measuring the structural connectivity between electrodes, and a graph convolution operation was implemented to characterize the spatiotemporal features of each channel. Fourthly, the Pearson's correlation coefficient and normalized mutual information of the EEG were computed to measure EEG functional connectivity, and a dynamic filtering module was used to generate sample-specific filters, and then these customized filters performed dynamic convolution on each sample. Finally, the output of the dynamic convolution was aggregated using 2D convolution to obtain the residual component, which was then added with the interpolated low-resolution EEG to obtain the high-resolution EEG. The experimental results showed that the SR model can effectively reconstruct high-density EEG with high performance and demonstrated its superiority to the original low-resolution EEG in ASD discrimination and spatial localization of ASD.

In summary, the CNN is able to effectively capture the spatio-

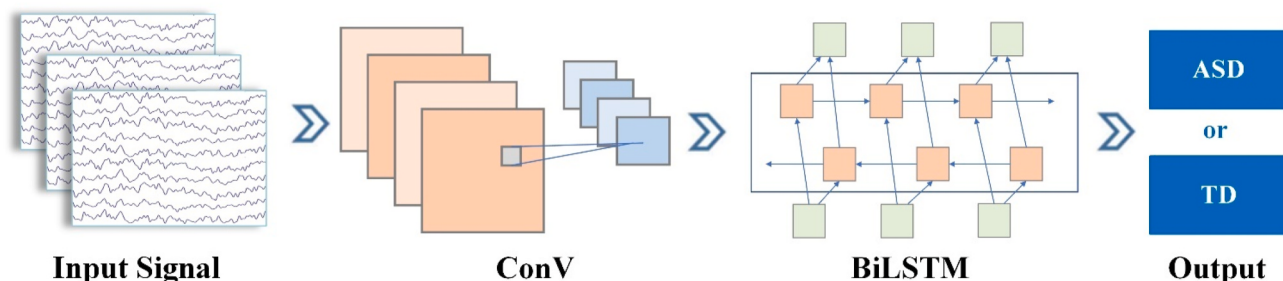
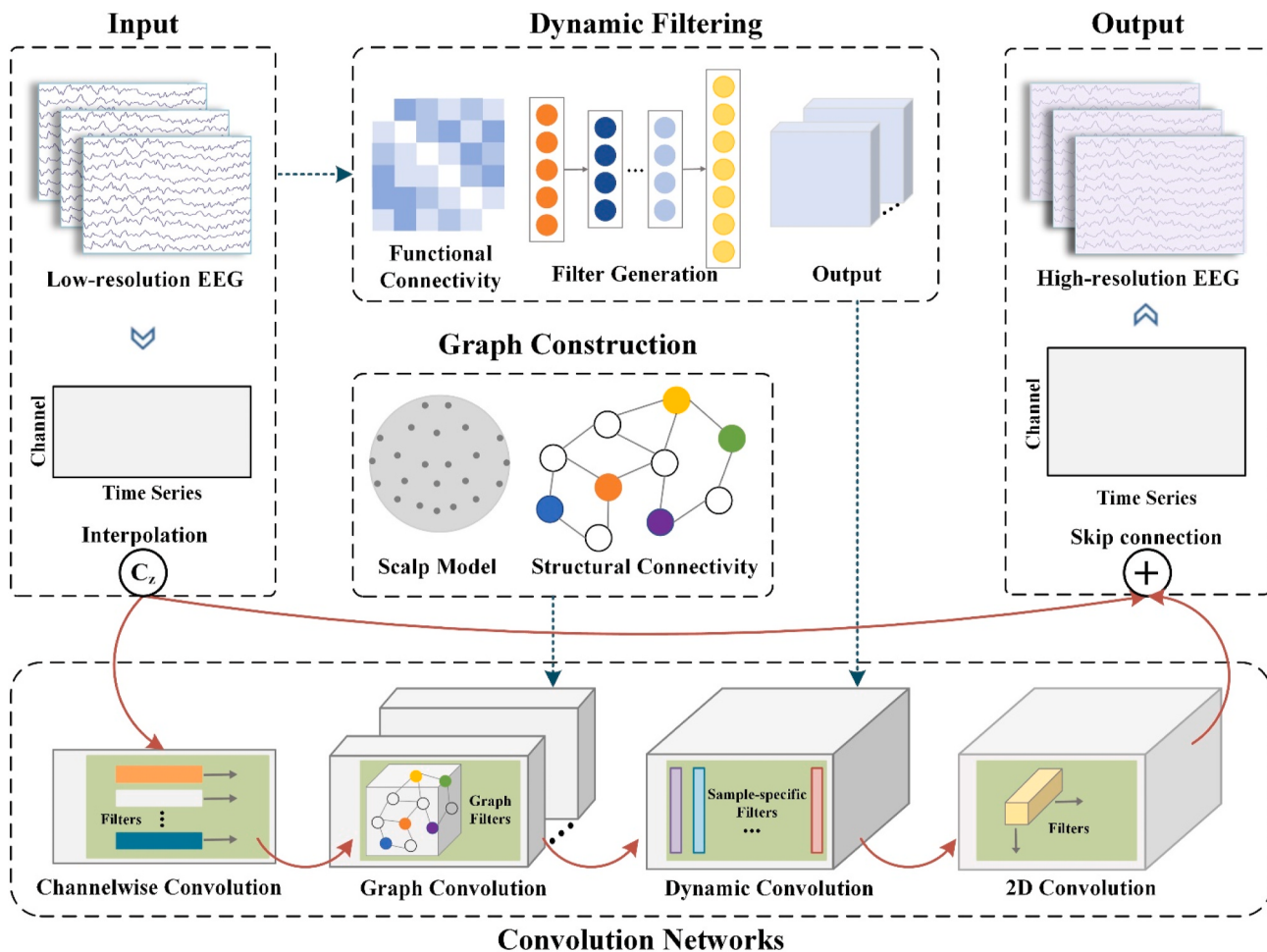


Fig. 16. CNN-BiLSTM based ASD identification [172].



**Fig. 17.** The GCN-based ASD identification [173].

temporal characteristics of EEG by extracting the local features of EEG signals using convolutional kernels. However, it performs relatively weakly in capturing the long-term dependence of sequential data. By contrast, the RNN is capable of accepting both current input data and previously received input data. Therefore, it is well-suited for handling time-series data. Nevertheless, the cyclic structure of RNN makes it face challenges such as gradient vanishing or explosion when dealing with long-term dependencies. The GCN is suitable for learning the representation of nodes in a graph, which can effectively capture the relationships between different brain regions, particularly in analyzing brain connectivity patterns. However, for larger or more complex graph structures, GCNs may exhibit higher computational complexity. Therefore, the choice of a neural network architecture for EEG signal analysis depends on the specific task and data characteristics. Combining the strengths of CNN, RNN, and GCN in a hybrid model can overcome the limitations of an individual network architecture, providing a more powerful solution for complex tasks.

#### 4.4. Summary

We summarize the deep learning methods for EEG-based ASD identification. Table 4 illustrates the dataset, the method, and the model performance of each study.

## 5. Multi-modal fusion-based methods

### 5.1. Autism diagnosis based on multimodal data

The existing ASD identification methods mainly relied on unimodal data, such as EEG, eye movement, facial expression, etc. However, ASD is a complex heterogeneous neurodevelopmental disorder, and it is difficult to accurately identify ASD solely by unimodal data such as EEG. Therefore, researchers have been combining physiological signals and external behavioral data to explore the heterogeneous characteristics of ASD, including EEG signals, eye tracking data, and facial expressions. As physiological signals, EEG can capture the electrical activity of brain neurons, reflecting the cognitive processes, thinking activities, and emotional states of individuals. Eye tracking data can record the eye movement of individuals, reflecting their external behavior and attention states. Facial expressions are one of the most important external behavioral signals in social interactions, which can convey emotions and intentions of individuals. The combination of internal physiological signals and external behavioral data can not only provide more accurate and personalized protocols for diagnosis, assessment, and treatment, but also help in understanding the etiology and pathogenesis of ASD. Therefore, in this review, we summarize the studies of autism identification based on multimodal fusion, including the combination of EEG and eye tracking, and the combination of EEG, eye tracking, and facial expression. As shown in Fig. 18, the multimodal fusion-based methods can be divided into three steps. First, the features are extracted separately from the input multimodal signals, e.g., EEG features can be extracted either manually or automatically using an autoencoder.

**Table 4**

Deep learning-based methods for ASD identification using EEG data. CNN: Convolutional Neural Network, DCNN: Deep Convolutional Neural Network, GCN: Graph Convolutional Network, LSTM: Long Short-term Memory Network, FC Layer: Fully-connected Layer.

Study	Dataset	Feature Extraction	Classification	Performance (%)
Ali et al. [180] 2020	8 ASD vs. 12 TD; 16 Channels; 256 Hz	CNN	FC Layer, Softmax	Accuracy = 80.00
Ranjani et al. [112] 2021	8 ASD vs. 12 epileptic vs. 18 TD; 16 Channels; 256Hz	Power Spectral Density Energy Map, DCNN	FC Layer	Accuracy = 80.00
Baygin et al. [179] 2021	61 ASD vs. 61 TD; 64 Channels, 500 Hz	Spectrogram Image, Pre- trained Model	Cubic SVM	Accuracy = 96.44 Sensitivity = 97.79 Specificity = 93.16 F1 Scores = 97.49
Tawhid et al. [155] 2021	12 ASD vs. 4 TD; 16 Channels, 256 Hz	Spectrogram Image, CNN	FC Layer, Softmax	Accuracy = 99.15 Sensitivity = 99.19 Specificity = 99.04 F1 Scores = 100
Ali et al. [171] 2021	39 ASD vs. 14 TD; 117Channels, 500 Hz	BiLSTM	FC Layer, Softmax	Accuracy = 99.6
Dong et al. [169] 2021	86 ASD vs. 98 TD; 8 Channels, 1000 Hz	Q-Learning, CNN	FC Layer, Sigmoid	Accuracy = 98.88 Sensitivity = 100 Specificity = 96.4 F1 Scores = 99.19
Ari et al. [156] 2022	20 ASD vs. 9 TD; 16 Channels, 256 Hz	EEG Rhythm Image, Extreme Learning Machine Autoencoder	Pre-trained CNN	Accuracy = 83.23
Ali te al [172]. 2022	39 ASD vs. 14 TD; 117Channels, 500 Hz	CNN BiLSTM	FC Layer	Accuracy = 97.70
Tang et al. [173] 2022	89 ASD vs. 121 TD; 62 Channels, 256 Hz	Deep EEG Super Resolution, Power Spectral Density	SVM	Accuracy = 96.97
Wadhera et al. [181] 2022	30 ASD vs. 30 TD; 256 Hz	Construction Graphs, Visible- GCN	FC Layer, Softmax	Accuracy = 93.78
ud-Din et al. [182] 2022	14 ASD vs. 14 TD;	Second-order Wavelet Scattering Transform, LSTM, CNN	FC Layer, Softmax	Accuracy (LSTM) = 94.00 Accuracy (CNN) = 92.00
Tawhid et al. [122] 2023	12 ASD vs. 4 TD; 16 Channels; 256Hz	Spectrograms Images, CNN	FC Layer, Softmax	Accuracy = 98.48 Sensitivity = 99.03 Specificity = 99.61

Second, the features of each modality are fused by simple integration, autoencoder-based fusion, or graph construction. Finally, appropriate classifiers are constructed based on the features to achieve accurate autism identification. Furthermore, in this review, we analyze and discuss five practical examples of multimodal-based autism identification, detailing how combining EEG data with other modalities can enhance the diagnosis of ASD.

Thapaliya et al. [87] made the first attempt to identify ASD using a combination of EEG and eye-tracking (ET) data. The dataset used in the study included 24 ASD children and 28 TD children, where EEG data were recorded from 128 channels at a sampling rate of 500 Hz and eye movement data were collected using a Tobii X50 eye tracker. Firstly, the data of the two modalities were preprocessed. Then, the features of the two modalities were extracted and concatenated. Finally, the fused features were sent to SVM, LR, DNN and Naive Bayes for classification, respectively. The experimental results showed that combining EEG with ET can improve the accuracy of ASD identification. Kang et al. [174] also adopted multi-modal fusion to diagnose ASD. First, power spectrum density (PSD) was performed to extract EEG frequency domain features. Second, children's gaze points at the face pictures were analyzed based on eye-tracking data to quantify children's engagement with each area of interest. Then, feature selection was performed on the EEG and ET features by the minimum-redundancy-maximum-relevance method to obtain the set of features with maximum relevance to the class label. Finally, these features were fed into the SVM for ASD identification. A total of 97 children aged 3–6 years were recruited in the study, including 49 ASD children and 48 TD children. EEG data were recorded from 128 channels at a sampling rate of 1000 Hz, and eye movement data were collected using a Tobii TX300 eye-tracking system. The method was validated on this dataset and achieves the accuracy of 85 % and the AUC of 93 %. The experimental results preliminarily proved that it is an effective method to diagnose ASD by combining EEG and ET data. However, as the method only concatenates the features of the two modalities and ignores the correlation between the original biological signals, it has certain limitations in multi-modal fusion for the diagnosis of ASD.

In order to fully exploit various correlations and complementarities provided by multi-modal data, Zhang et al. [175] proposed a joint analysis approach of EEG and ET for children ASD evaluation, which focuses on deep fusion of the features in two modalities. First, the synchronization measure, information entropy, and time-frequency features of multi-channel EEG signals were calculated for EEG signals. The time information such as total fixation duration on certain AOI was recorded to quantify each child's engagement for each AOI, and the most important ET features were selected using the random forest. Then, a feature graph was constructed for each sample, where EEG features and ET features were defined as nodes of the graph, and the covariance between the features was used as edges between nodes in the graph. Finally, a GCN model with 2 hidden layers was used to implicitly fuse the feature graphs and differentiate the children with ASD from the TD subjects. The dataset was experimented on two types of biological signals collected from 42 children (21 ASD and 21 TD subjects, 3–6 years old), in which EEG signals were collected from 128 channels at a sampling rate of 1000HZ, and the ET data were collected by an eye tracking system with a sampling rate of 300Hz. Experimental results showed that the method can achieve the accuracy of 95 % in ASD detection, proving that there is also a strong correlation between two biosignals collected asynchronously. Han et al. [176] also designed a two-step multi-modal learning approach based on stacked denoising autoencoder for the fusion of multi-modal information. Firstly, the features of relative power energy, multiscale entropy and functional connectivity were extracted to highlight the characteristics of EEG signals associated with ASD. Six statistical metrics of ET, including time to first fixation, fixations before, total fixation duration, fixation count, fixation duration, and visit count, were extracted to initially characterize the ET data. Afterwards, to reduce the high-dimensionality and redundancy of the extracted initial

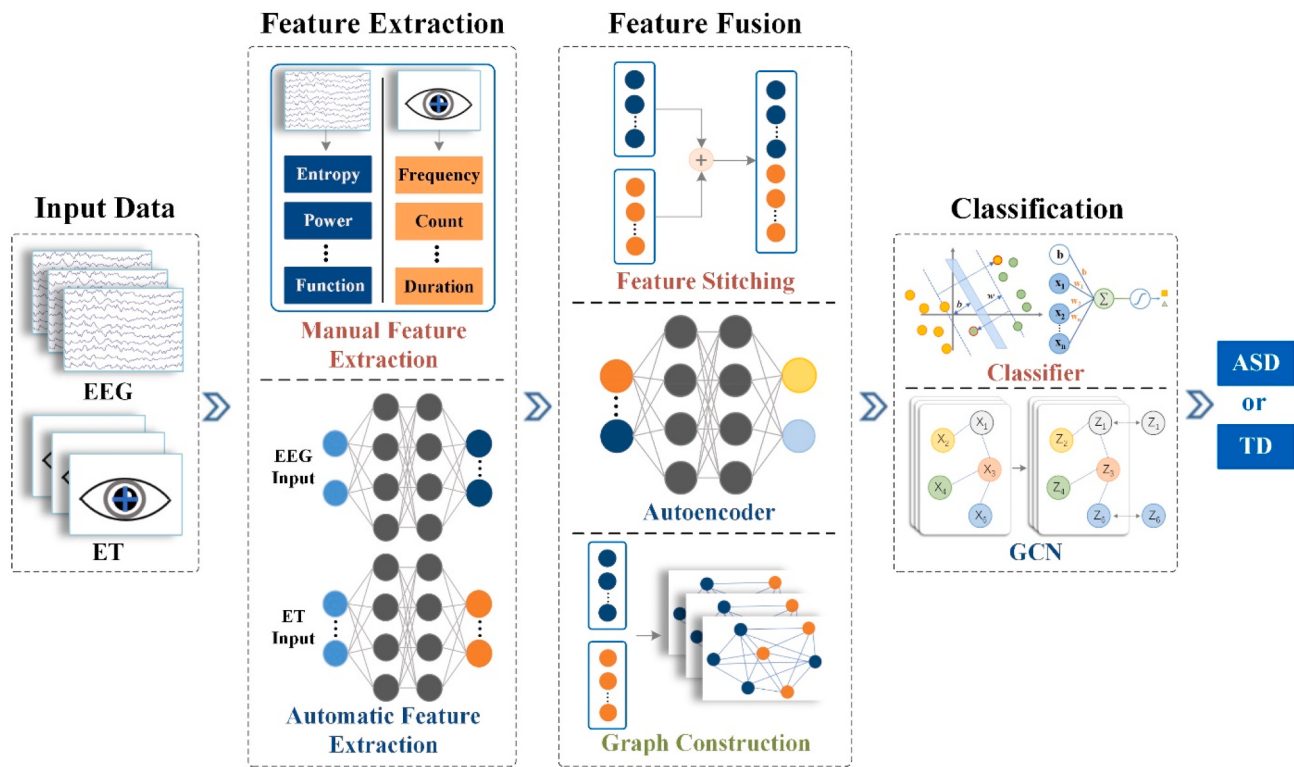


**Fig. 18.** Multi-modal fusion-based methods [176].

EEG and ET features, two stacked denoising autoencoders (SDAE) were designed for feature learning of EEG and ET data, respectively. Finally, through a third SDAE model, the EEG and ET features are fused to learn the relationship between EEG-based high-level representations and ET-based high-level representations, and ASD identification. The dataset used in this study contained 90 subjects, including 40 ASD children and 50 TD children aged 3–6 years. The EEG signals were recorded with a high-density array of 128 Ag/AgCl passive electrodes (Electrical Geodesics Inc., EGI) at a sampling rate of 1000 Hz. The ET data were recorded using a Tobii TX300 eye tracker with a sampling frequency of 300 Hz. Experimental results showed that this method combining EEG and ET data can achieve more effective ASD diagnosis.

Zhang et al. [177] argued that multi-modal fusion should not only fully characterize the interaction relationship of different modal features, but also the individuality of subjects should also be highlighted in the derived structural relationships [177]. Therefore, they proposed a graph-based solution to the above challenges by constructing the relationship between bimodal features of EEG signals and eye movement data for personalized assessment of ASD subjects. Firstly, the EEG features and the ET features are extracted separately to obtain bimodal features. Secondly, the dual-modal features were mapped to the sample-specific graphs using a shallow MLP-based coding module. Then, the GCN was applied to the sample-specific graphs, aiming to fuse the global information of the dual-modal features and learn the corresponding feature relationship with the goal of adapting to the subject individuality. The study was validated on a dataset from Beijing Normal University. This dataset asynchronously recorded eye movement data and EEG signals of 64 children (3–6 years old), in which EEG signals were collected in 128 channels at a sampling rate of 250Hz; ET data were collected at a sampling rate of 300Hz. Each subject was collected seven times. The proposed method achieved higher performance than other multimodal fusion methods in ASD assessment, with an accuracy rate of 99.73 %. Moreover, it can characterize the interaction relationship of different modal features and can better adapt to individual differences.

In addition to the fusion of EEG and ET data for ASD identification, Liao et al. [178] proposed a three-modal fusion method of eye fixation, facial expression and EEG data, which contains three steps, i.e., feature extraction, feature fusion and classification. For feature extraction, firstly, the K-means algorithm was used to cluster the gaze points and classify different regions of interest; secondly, a facial expression recognition based on CNN and soft label was designed to count the number of target expressions in every 40 frames; finally, the FFT was used to obtain five frequency bands and the power in each band was extracted. For feature fusion, a hybrid fusion framework based on a weighted naive Bayes algorithm was proposed for multi-modal data fusion. For classification, three commonly classifiers are used, including RF, SVM and KNN. The study collected three-modal data from 40 children with ASD and 40 children with TD by Tobii eye tracker, video camera, and Emotiv EPOC+. The results showed that combining complementary information of three-modal data could obtain a highest accuracy of 87.50 %. They also found that eye fixation, facial expression, and EEG had different discriminative power for ASD and TD, and indicated that EEG may be the most discriminative information compared to eye gaze and facial expression.

## 5.2. Summary

We summarize the multi-modal fusion methods for EEG-based ASD identification. Table 5 illustrates the dataset, the method, and the model performance of each study.

## 6. Conclusion & discussion of opportunities and challenges

In this review, we summarize recent achievements of traditional machine learning and deep learning architectures in identifying ASD children from EEG data. For traditional machine learning methods, it introduces the tasks and common methods of each stage according to the workflow. It also introduces denoising techniques commonly used in the data preprocessing stage and popular EEG data preprocessing tools.

**Table 5**

Multi-modal fusion methods for ASD identification. PCA: Principal Component Analysis, SVM: Support Vector Machine, AOI: Areas of Interest, DNN: Deep Neural Network, NB: Naive Bayes, MRMR: Minimum Redundancy Maximum Relevance, AUC: Area under Curve, GCN: Graph Convolutional Network, SNRA: Stacked Noise Reduction Autoencoder, FC Layer: Fully-connected Layer, FFT: Fast Fourier Transform.

Study	Dataset	Feature Extraction	Feature Fusion	Classification	Performance (%)
Thapaliya et al. [87] 2018	34 Subjects; 128 Channels; 500 Hz; Tobi X50	Statistical Features, Entropy, Fixation Time	PCA, Feature Concatenation	SVM, Logistic, DNN, Gaussian NB	Accuracy = 100
Kang et al. [174] 2020	49 ASD vs. 48 TD; 128 Channel; 1000 Hz; TX300	Power Spectrum, Fixation Time in AOI	MRMR, Feature Concatenation	SVM	Accuracy = 85.00 AUC = 93.00
Zhang et al. [175] 2021	21 ASD vs. 21 TD; 8 Channels; 1000 Hz; 300 Hz ET	Entropy, Functional Connectivity, Fixation Time in AOI	Random Forest, Feature Graph	GCN	Accuracy = 95.00
Han et al. [176] 2022	40 ASD vs. 50 TD; 62 Channels; 256 Hz; 300 Hz ET	Two SNRAs	SNRA	SNRA	Accuracy = 95.56 Sensitivity = 92.50 Specificity = 98.00
Zhang et al. [177] 2023	32 ASD vs. 32TD; 128 Channels; 250 Hz; 300 Hz ET	Band Information, Manual Extraction	Sample-specific Graph, Deep-GCN	FC Layer, Sigmoid	Accuracy = 99.73
Liao et al. [178] 2022	40 ASD vs. 30TD; Tobii Eye Tracker; video camera; Emotiv EPOC+	FFT, Frequency of Fixation Points in AOI, CNN	Weighted NB	RF, SVM, KNN	Accuracy = 87.50

Then, it describes the feature analysis methods used in the feature extraction stage, including time-domain analysis, frequency-domain analysis, time-frequency analysis. For classification, 5 classifiers commonly used are reviewed. For deep learning methods, it analyzes several existing methods according to different network architectures, including convolutional neural network-based, recurrent neural network-based, and graph convolutional network-based methods. In addition, it also reviews multi-modal fusion methods for identifying autism.

On the whole, traditional machine learning methods usually rely on manually extracted features. They usually perform better when analyzing small sample sizes of EEG data and the model interpretability is relatively high, but they fail to capture the complex relationships hidden in the raw data. In contrast, deep learning methods are able to automatically learn the feature representations in the raw data without the need to extract features manually. When analyzing large-scale datasets, they can discover hidden patterns and complex associations in the data, thus achieving better performance in EEG-based ASD identification. At present, traditional machine learning methods have been used more widely than deep learning methods. One of the very important reasons is due to the small scale of the EEG dataset for autism. After preprocessing and feature extraction on a small-scale dataset, accurate classification can be achieved using traditional classifiers. By contrast, deep learning requires a large amount of data for training to achieve good performance. Therefore, when there is a sufficient amount of data, the performance of deep learning in autism diagnosis will be significantly improved, showing greater potential. In recent years, a study [183] has proposed a non-invasive temperature sensation method to train amputees to sense temperature with psychophysical sensory substitution, i.e., using visual feedback of different colors to make the amputees perceive temperature. This suggests that innovations in rehabilitation technology are not limited to physical health, but also play a role in mental health and rehabilitation of specific groups, such as children with autism. In future research, new opportunities and challenges will emerge to promote the development of more interpretable, intelligent, and accurate ASD identification tools. This will be expected to improve the early diagnosis of children with ASD, promote personalized treatment, and potentially make significant breakthroughs in understanding the underlying pathophysiology of ASD.

#### A. Deep learning-based EEG de-artifacting.

EEG recordings are prone to various artifacts, such as eye blinks and muscle activity that can interfere with the underlying neural signals relevant to ASD. Therefore, an essential step to deal with EEG data is to remove these artifacts. Traditional de-artifacting methods, while widely used, have some inherent inconveniences since they usually rely on predefined rules to identify and remove artifacts. These methods require a priori knowledge of the artifact characteristics, and are not adaptable to a wide variety of datasets and less effective in handling complex or novel types of artifacts. Additionally, traditional methods may involve multiple preprocessing steps, making the overall process time-consuming and less amenable to real-time applications. To overcome these inconveniences, there is a growing interest in exploring deep learning-based EEG artifact removal techniques based on self-attention mechanism, which can focus on electrical waves generated by neural activity in the brain and assign different weights to different channels, time segments, or frequency bands of EEG signals and help detect brain regions associated with artifacts. Deep learning-based EEG de-artifacting not only can process high-noise EEG data, but also help improve the efficiency of ASD diagnosis.

#### B. EEG data augmentation.

Due to the complexity and particularity of medical data and the sensitivity and privacy of ASD children's, there are very few publicly-available EEG datasets for ASD identification. Most of the studies covered in this review used self-collected EEG datasets, resulting in the majority of findings not being directly comparable, which hinders the development of ASD identification methods. In addition, current EEG datasets are usually small, which is often insufficient to meet the data requirements of deep learning, limiting the use and development of deep learning methods. Therefore, introducing data augmentation techniques into ASD diagnosis using EEG signals holds significant potential for enhancing the performance, robustness, and generalization ability of deep learning models. For example, we can use generative models, such as generative adversarial networks (GAN), variational auto-encoders (VAE) and diffusion models to augment the EEG dataset. The GAN consists of a generator and a discriminator. The generator creates

synthetic data, while the discriminator tries to differentiate between real and generated data. The GAN can be used to generate EEG samples similar to the real EEG signals. The VAE consists of an encoder that maps EEG data to a distribution in the latent space and a decoder that generates EEG data from the latent space. It can learn the spatio-temporal features of EEG signals, thus generating diverse but realistic samples. The diffusion model describes the evolution of a probability distribution over time, which can capture the temporal dependence more accurately by modeling the temporal evolution of the EEG signals, so that the generated EEG samples are more consistent with the real EEG signals. The goal of employing these data augmentation methods is not only to increase the size of the training set but also to enable deep learning models to learn a diverse range of EEG patterns, improving its ability to generalize across different individuals and conditions.

#### C. Exploring interpretable models for ASD diagnosis.

The Artificial Intelligence (AI)-based technologies for ASD diagnosis is gathering increasing attention, which can translate scientific research into practical applications. Model interpretability is important for disease diagnosis since strong interpretability enhances the trust among doctors, patients and AI systems. At the same time, it can offer insights into how the network model processes information, aiding in the optimization of autism diagnostic models and guiding future data acquisition. In addition, it can further help reveal the underlying physiological characteristics of autism and provide a diagnostic basis for medical professionals. However, in deep learning, black-box models can only offer either a "yes" or "no" diagnosis without providing an interpretation of the underlying factors contributing to the ASD diagnosis. For that, it is important to incorporate clinical knowledge into the development of new interpretable deep learning approaches for ASD diagnosis. This ensures that the decisions made by the models can align with clinical consensus and meet the specific needs of the AI-aided autism diagnosis. This combination between AI and medical expertise not only increases the level of trust but also enhances the utility and reliability of deep learning models within the healthcare domain. Moreover, the interpretability of deep learning models can be enhanced by improving the models themselves. For instance, by introducing the layer-wise attention method, the attention weights of different layers can be visualized. This can help reveal the way that the model integrates information of brain regions or frequency bands, and the rationale behind the model's predictions.

#### D. Multimodal fusion-based autism diagnosis.

The ASD is a complex heterogeneous neurodevelopmental disorder, and it is difficult to make a complete assessment of ASD only based on unimodal data such as EEG. Therefore, rather than using uni-modal data, e.g., EEG, facial expression (FE) and eye tracking (ET), more and more researches have applied multi-modal data (e.g., EEG + ET, EEG + ET + FE) to obtain accurate identification. Furthermore, multi-modal fusion not only improves the diagnostic accuracy of ASD, but also provides the possibility to explore hidden relationships and unrevealed pathological mechanisms from real-world data. While multi-modal data can offer a wealth of information, the presence of redundancy and noise within the data presents challenges for autism identification. Therefore, it is important to design an effective fusion model that can adaptively fuse the features according to the characteristics and correlations of data from different modalities, and thus achieve more effective and efficient autism identification. For example, in feature-level fusion, graph convolutional neural networks can be utilized to model complex relationships between multimodal data and enhance important information. In decision-level fusion, ensemble learning can be used to integrate predictions from different models to improve the overall performance. For ASD diagnosis, effective multimodal fusion methods can help reveal the associations between behavioral manifestations with neural

mechanisms of autism.

#### E. Assessing the severity of autism.

The symptom severity, language skills, intellectual ability, and medical conditions may vary widely among individuals with ASD. Current research for ASD identification generally believes that there are three severity levels of ASD, which are Level 1 "Requiring Support", Level 2 "Requiring Substantial Support", and Level 3 "Requiring Very Substantial Support". With the prevalence increase, assessing the severity of autism becomes increasingly meaningful since it helps individualize the diagnosis and treatment of children with ASD. Additionally, it explores the underlying phenotypic heterogeneity of autism spectrum disorders. However, the imbalance in the number of samples and the time-consuming process of labeling categories for ASD children limit the learning and representation capabilities of the deep learning models. Therefore, it is necessary to recruit ASD children of varying severity and record their behaviors. In the absence of labeled severity levels, the EEG data of all the subjects can be adaptively clustered into several groups in an unsupervised manner, which provides the possibility for the assessment of autism severity. For example, graph-based clustering algorithms can be used via constructing a similarity graph between the subjects. This will help identify common characteristics of ASD and infer the specificity of EEG signals, thus better assessing different manifestations and severity of autism.

#### CRediT authorship contribution statement

**Jing Li:** Conceptualization, Funding acquisition, Investigation, Methodology, Writing – original draft, Writing – review & editing. **Xiaoli Kong:** Conceptualization, Methodology, Writing – original draft, Writing – review & editing. **Linlin Sun:** Investigation, Methodology, Writing – original draft, Writing – review & editing. **Xu Chen:** Conceptualization, Writing – original draft, Writing – review & editing. **Gaoxiang Ouyang:** Conceptualization, Investigation, Methodology, Writing – original draft, Writing – review & editing. **Xiaoli Li:** Writing – original draft, Writing – review & editing. **Shengyong Chen:** Writing – original draft, Writing – review & editing.

#### Declaration of competing interest

None Declared.

#### Acknowledgement

This work was supported by National Natural Science Foundation of China under Grant 62373280 and 61963027.

#### References

- [1] G. Brihadiswaran, D. Haputhanthri, S. Gunathilaka, D. Meedeniya, S. Jayarathna, EEG-based processing and classification methodologies for autism spectrum disorder: a review, *J. Comput. Sci.* 15 (8) (2019) 1161–1183.
- [2] L. Duan, J.X. Liu, H.M. Yin, W.H. Wang, L. Liu, J.L. Shen, Z.D. Wang, Dynamic changes in spatiotemporal transcriptome reveal maternal immune dysregulation of autism spectrum disorder, *Comput. Biol. Med.* 151 (2022) 106334.
- [3] L. e Zwaigenbaum, M.L. Bauman, R. Choueiri, C. Kasari, A. Carter, D. Granpeesheh, Z. Mailloux, S.S. Roley, S. Wagner, D. Fein, K. Pierce, T. Buie, P. A. Davis, C. Newschaffer, D. Robins, A. Wetherby, W.L. Stone, N. Yirmiya, A. Estes, R.L. Hansen, J.C. McPartland, M.R. Natowicz, Early intervention for children with autism spectrum disorder under 3 years of age: recommendations for practice and research, *Pediatrics* 13 (1) (2015) 60–81.
- [4] N. Gabbay-Dizdar, M. Ilan, G. Meiri, M. Faroy, A. Michaelovski, H. Flusser, I. Menashe, J. Koller, D.A. Zachor, I. Dinstein, Early diagnosis of autism in the community is associated with marked improvement in social symptoms within 1–2 years, *Autism* 26 (6) (2022) 1353–1363.
- [5] M.C. Lai, M.V. Lombardo, S.B. Cohen, Autism, *Lancet* 383 (9920) (2014) 896–910.
- [6] E. Schopler, M.E.V. Bourgondien, G.J. Wellman, S.R. Love, Childhood Autism Rating Scale—Second Edition (CARS-2), Western Psychological Services, Los Angeles, CA, 2010.

- [7] C. Lord, R.J. Luyster, K. Gotham, W. Guthrie, Autism Diagnostic Observation Schedule, (ADOS-2), Part II: Toddler Module, second ed., Western Psychological Services, Los Angeles, 2012.
- [8] M. Khawaja, D. Robins, Checklist for Autism in Toddlers (CHAT), Encyclopedia of Autism Spectrum Disorders, Springer, New York, NY, 2013.
- [9] M. Rutter, A. Lecoutre, C. Lord, Autism Diagnostic Interview-Revised, vol. 29, Western Psychological Services, Los Angeles, CA, 2003, p. 30.
- [10] J.M.M. Torres, T. Clarkson, K.M. Hauschild, C.C. Luhmann, M.D. Lerner, G. Riccardi, Facial emotions are accurately encoded in the neural signal of those with autism spectrum disorder: a deep learning approach, *Biol. Psychiatr.: Cognitive Neuroscience and Neuroimaging* 7 (7) (2022) 688–695.
- [11] M. Schulte-Rüther, T. Kulvicius, S. Stroth, N. Wolff, V. Roessner, P.B. Marschik, I. Kamp-Becker, L. Poustka, Using machine learning to improve diagnostic assessment of ASD in the light of specific differential and co-occurring Diagnoses, *JCPP (J. Child Psychol. Psychiatry)* 64 (1) (2023) 16–26.
- [12] Z.Q. Chang, J.M.D. Martino, R. Aiello, J. Baker, K. Carpenter, S. Compton, N. Davis, B. Eichner, S. Espinosa, J. Flowers, L. Franz, A. Harris, J. Howard, S. Perochon, E.M. Perrin, P.R.K. Babu, M. Spanos, C. Sullivan, B.K. Walter, S. H. Kollins, G. Dawson, G. Sapiro, Computational methods to measure patterns of gaze in toddlers with autism spectrum disorder, *JAMA Pediatr.* 175 (8) (2021) 827–836.
- [13] J. Li, Z.J. Chen, Y.H. Zhong, H.K. Lam, J.X. Han, G.X. Ouyang, X.L. Li, H.H. Liu, Appearance-based gaze estimation for ASD diagnosis, *IEEE Trans. Cybern.* 52 (7) (2022) 6504–6517.
- [14] Z. Zhao, J.W. Wei, J.Y. Xing, X.B. Zhang, X.D. Qu, X.Y. Hu, J.P. Lu, Use of oculomotor behavior to classify ASD children and typical development: a novel implementation of the machine learning approach, *J. Autism Dev. Disord.* 53 (3) (2023) 934–946.
- [15] A. Gaspar, D. Oliva, S. Hinojosa, I. Aranguren, D. Zaldivar, An optimized kernel extreme learning machine for the classification of the autism spectrum disorder by using gaze tracking images, *Appl. Soft Comput.* 120 (2022) 108654.
- [16] A. Pradhan, V. Chester, K. Padhiar, Classification of autism and control gait in children using multisegment foot kinematic features, *Bioengineering* 9 (10) (2022) 552.
- [17] N.K. Zakaria, N.M. Tahir, R. Jailania, M.M. Taher, Anomaly gait detection in ASD children based on markerless-based gait features, *Journal Kejuruteraan* 34 (5) (2022) 965–973.
- [18] J. Li, Z.J. Chen, G.F. Li, G.X. Ouyang, X.L. Li, Automatic classification of ASD children using appearance-based features from videos, *Neurocomputing* 470 (2022) 40–50.
- [19] J.H. Yu, H.W. Gao, D.L. Zhou, J.G. Liu, Q. Gao, Z.J. Ju, Deep temporal model-based identity-aware hand detection for space human–robot interaction, *IEEE Trans. Cybern.* 52 (12) (2021) 13738–13751.
- [20] J.J. Liu, Z.Y. Wang, Z. Xu, B. Ji, G.Y. Zhang, Y. Wang, J.X. Deng, Q. Xu, X. Xu, H.H. Liu, Early screening of autism in toddlers via response-to-instructions protocol, *IEEE Trans. Cybern.* 52 (5) (2020) 3914–3924.
- [21] Z.Y. Wang, J.J. Liu, K.S. He, Q. Xu, X. Xu, H.H. Liu, Screening early ASD children spectrum disorder via response-to-name protocol, *IEEE Trans. Ind. Inf.* 17 (1) (2021) 587–595.
- [22] A.K. Subudhi, M. Mohanty, S.K. Sahoo, S.K. Mohanty, B. Mohanty, Automated delimitation and classification of autistic disorder using EEG signal, *IETE J. Res.* 69 (2) (2023) 951–959.
- [23] F.L. Li, S. Zhang, L. Jiang, K.Y. Duan, R. Feng, Y.L. Zhang, G. Zhang, Y.S. Zhang, P.Y. Li, D.Z. Yao, J. Xie, W.M. Xu, P. Xu, Recognition of Autism Spectrum Disorder in Children Based on Electroencephalogram Network Topology, *Cognitive Neurodynamics*, 2023, pp. 1–13.
- [24] X.X. Li, Y. Zhou, N. Dvornek, M.H. Zhang, S.Y. Gao, J.T. Zhuang, D. Scheinost, L. H. Staib, P. Ventola, J.S. Duncan, BrainGNN: interpretable brain graph neural network for fMRI analysis, *Med. Image Anal.* 74 (2021) 102233.
- [25] M.R. Ahmed, Y. Zhang, Y. Liu, H.G. Liao, Single volume image generator and deep learning-based ASD classification, *IEEE Journal of Biomedical and Health Informatics* 24 (11) (2020) 3044–3054.
- [26] M. Kangani-Farahani, M.A. Maliki, J.G. Zwicker, Motor impairments in children with autism spectrum disorder: a systematic review and meta-analysis, *J. Autism Dev. Disord.* (2023) 1–21.
- [27] P. Singh, P. Malhi, Early diagnosis of autism spectrum disorder: what the pediatricians should know, *Indian Journal of Pediatrics* volume 90 (4) (2023) 364–368.
- [28] M.L. Bauman, T.L. Kemper, Neuroanatomic observations of the brain in autism: a review and future directions, *Int. J. Dev. Neurosci.* 23 (2–3) (2005) 183–187.
- [29] K. Garbett, P.J. Ebert, A. Mitchell, C. Lintas, B. Manzi, K. Mirmics, A.M. Persico, Immune transcriptome alterations in the temporal cortex of subjects with autism, *Neurobiol. Dis.* 30 (3) (2008) 303–311.
- [30] C. Scuderi, A. Verkhratsky, The role of neuroglia in autism spectrum disorders, *Molecular Biology and Translational Science* 173 (2020) 301–330.
- [31] J.M. Soares, R. Magalhães, P.S. Moreira, A. Sousa, E. Ganz, A. Sampao, V. Alves, P. Marques, N. Sousa, A hitchhiker's guide to functional magnetic resonance imaging, *Front. Neurosci.* 10 (2016) 515.
- [32] G.Q. Wen, P. Cao, H.W. Bao, W.J. Yang, T. Zheng, O. Zaiane, Mvs-Gen, A prior brain structure learning-guided multi-view graph convolution network for autism spectrum disorder diagnosis, *Comput. Biol. Med.* (142) (2022) 105239.
- [33] H.D. Frank, S.A. Marilyn, M. Gloria, J.G. Arthur, Age-related differences in brain electrical activity of healthy subjects, *Ann. Neurol.* 16 (4) (1984) 430–438.
- [34] J. Wang, J. Barstein, L.E. Ethridge, M.W. Mosconi, Y. Takarae, J.A. Sweeney, Resting state EEG abnormalities in autism spectrum disorders, *J. Neurodev. Disord.* 5 (1) (2013) 1–14.
- [35] W.L. Wang, F.F. Qi, D.P. Wipf, C. Cai, T.Y. Yu, Y.Q. Li, Y. Zhang, Z.L. Yu, W. Wu, Sparse Bayesian learning for end-to-end EEG decoding, *IEEE Trans. Pattern Anal. Mach. Intell.* 45 (12) (2023) 15632–15649.
- [36] S. Raziani, S. Ahmadian, S.M.J. Jalali, A. Chalechale, An efficient hybrid model based on modified whale optimization algorithm and multilayer perceptron neural network for medical classification problems, *JBE* 19 (2022) 1504–1521.
- [37] J.W. Britton, L.C. Frey, J.L. Hopp, M.Z. Koubeissi, W.E. Lievens, E.M. Pestana-Knight, E.K.S. Louis, *Electroencephalography (EEG): an Introductory Text and Atlas of Normal and Abnormal Findings in Adults*, American Epilepsy Society, 2016 27748095.
- [38] T.F. Song, W.M. Zheng, P. Song, Z. Cui, EEG emotion recognition using dynamical graph convolutional neural networks, *IEEE Transactions on Affective Computing* 11 (3) (2020) 532–541.
- [39] S.Q. Liu, X. Wang, L. Zhao, B. Li, W.M. Hu, J. Yu, Y.D. Zhang, 3DCANN: a spatio-temporal convolution attention neural network for EEG emotion recognition, *IEEE Journal of Biomedical and Health Informatics* 26 (11) (2022) 5321–5331.
- [40] X.Q. Li, P.H. Li, Z. Fang, Z.D. Fang, L.L. Cheng, Z.Y. Wang, W.J. Wang, Research on EEG emotion recognition based on CNN+ BiLSTM+ self-attention model, *Optoelectron. Lett.* 19 (8) (2023) 506–512.
- [41] S.D. Wang, H. Gu, Q.L. Yao, C. Yang, X.L. Li, G.X. Ouyang, Task-independent auditory probes reveal changes in mental workload during simulated quadrotor UAV training, *Health Inf. Sci. Syst.* 11 (2023) 12.
- [42] X. Zhang, L.N. Yao, M.Q. Dong, Z. Liu, Y. Zhang, Y. Li, Adversarial representation learning for robust patient-independent epileptic seizure detection, *IEEE Journal of Biomedical and Health Informatics* 24 (10) (2020) 2852–2859.
- [43] A. Yasuhara, Correlation between EEG abnormalities and symptoms of autism spectrum disorder (ASD), *Brain Dev.* 32 (10) (2010) 791–798.
- [44] L.M. Oberman, E.M. Hubbard, J.P. McCleery, E.L. Altschuler, V.S. Ramachandran, J.A. Pineda, EEG evidence for mirror neuron dysfunction in autism spectrum disorders, *Cognit. Brain Res.* 24 (2) (2005) 190–198.
- [45] J.M. Peters, M. Taquet, C. Vega, S.S. Jeste, I.S. Fernández, J. Tan, C.A. Nelson, M. Sahin, S.K. Warfield, Brain functional networks in syndromic and non-syndromic autism: a graph theoretical study of EEG connectivity, *BMC Med.* 11 (1) (2013) 1–16.
- [46] S.J. Webb, A.J. Naples, A.R. Levin, G. Hellermann, H. Borland, J. Benton, C. Carlos, T. McAllister, M. Santhosh, H. Seow, A. Atyabi, R. Bernier, K. Chawarska, G. Dawson, J. Dziura, S. Faja, S. Jeste, M. Murias, C.A. Nelson, M. Sabatos-DeVito, D. Senturk, F. Shic, C.A. Sugar, J.C. McParland, The autism biomarkers consortium for clinical trials: initial evaluation of a battery of candidate EEG biomarkers, *Am. J. Psychiatr.* 180 (1) (2023) 41–49.
- [47] M.J. Alhaddad, M.I. Kamel, H.M. Malibar, E.A. Alsaggaf, K. Thabit, F. Dahlwi, A. A. Hadi, Diagnosis autism by Fisher linear discriminant analysis FLDA via EEG, *International Journal of Bio-Science and Bio-Technology* 4 (2) (2012) 45–54.
- [48] W.J. Bosl, A. Tierney, H. Tager-Flusberg, C. Nelson, EEG complexity as a biomarker for autism spectrum disorder risk, *BMC Med.* 9 (2011) 18.
- [49] M. Khodatars, A. Shoeibi, D. Sadeghi, N. Ghaasemi, M. Jafari, P. Moridian, A. Khadem, R. Alizadehsani, A. Zare, Y.N. Kong, A. Khosravi, S. Nahavandi, S. Hussain, U. Acharya, M. Berk, Deep learning for neuroimaging-based diagnosis and rehabilitation of Autism Spectrum Disorder: a review, *Comput. Biol. Med.* 139 (2021) 104949.
- [50] C.M. Parlett-Pelleriti, E. Stevens, D. Dixon, E.J. Linstead, Applications of unsupervised machine learning in autism spectrum disorder research: a review, *Review Journal of Autism and Developmental Disorders* 10 (2023) 406–421.
- [51] S. Das, R. Zomorodi, M. Mirjalili, M. Kirkovski, D.M. Blumberger, T.K. Rajji, P. Desarkar, Machine learning approaches for electroencephalography and magnetoencephalography analyses in autism spectrum disorder: a systematic review, *Prog. Neuro Psychopharmacol. Biol. Psychiatr.* 123 (2023) 110705.
- [52] A. Liberati, D.G. Altman, J. Tetzlaff, C. Mulrow, P.C. Götzsche, J.P.A. Ioannidis, M. Clarke, P.J. Devereaux, J. Kleijnen, D. Moher, The PRISMA statement for reporting systematic reviews and meta-analyses of studies that evaluate health care interventions: explanation and elaboration, *Annals of Internal Medicine* 151 (4) (2009). W-65-W-94.
- [53] M.J. Alhaddad, M.I. Kamel, H.M. Malibar, E.A. Alsaggaf, K. Thabit, F. Dahlwi, A. A. Hadi, Diagnosis autism by Fisher linear discriminant analysis FLDA via EEG, *International Journal of Bio-Science and Bio-Technology* 4 (2) (2012) 45–54.
- [54] M. Ahmadlou, H. Adeli, and A. Adeli, Fuzzy synchronization likelihood-wavelet methodology for diagnosis of autism spectrum disorder, *J. Neurosci. Methods*, 211 (2) (2012) 203–209.
- [55] W.J. Bosl, H. Tager-Flusberg, C.A. Nelson, EEG analytics for early detection of autism spectrum disorder: a data-driven approach, *Sci. Rep.* 8 (1) (2018) 6828.
- [56] C.J. Honey, O. Sporns, L. Cammoun, P. Hagmann, Predicting human resting-state functional connectivity from structural connectivity, *Proc. Natl. Acad. Sci. USA* 106 (6) (2009) 2035–2040.
- [57] A. Shoka, M. Dessouky, A. El-Sherbeny, A. El-Sayed, Literature review on EEG preprocessing, feature extraction, and classifications techniques, *International Conference on Electronic Engineering* 28 (1) (2019) 292–299.
- [58] T.P. Jung, C. Humphries, T.W. Lee, S. Makeig, M. McKeown, V. Iragui, T. J. Sejnowski, Extended ICA removes artifacts from electroencephalographic recordings, *Adv. Neural Inf. Process. Syst.* 10 (1997) 894–900.
- [59] J.A. Uriagué, B. García-Zapirain, EEG artifact removal—state-of-the-art and guidelines, *J. Neural. Eng.* 12 (3) (2015) 031001.
- [60] D. Cosandier-Rimélé, J.M. Badier, P. Chauvel, F. Wendling, A physiologically plausible spatio-temporal model for EEG signals recorded with intracerebral electrodes in human partial epilepsy, *IEEE (Inst. Electr. Electron. Eng.) Trans. Biomed. Eng.* 54 (3) (2007) 380–388.

- [61] P. Comon, Independent component analysis.A new concept, *Signal Process.* 36 (3) (1994) 287–314.
- [62] T.P. Jung, S. Makeig, C. Humphries, T.W. Lee, M.J. McKeown, V. Iragui, T. J. Sejnowski, Removing electroencephalographic artifacts by blind source separation, *Psychophysiology* 37 (2) (2000) 163–178.
- [63] S. Choi, A. Cichocki, H.M. Park, S.Y. Lee, Blind source separation and independent component analysis: a review, *Neural Information Processing-Letters and Reviews* 6 (1) (2016) 1–57.
- [64] M. Iwashashi, H. Arof, P. Cumming, N. Mokhtar, C.Y. Sai, Automated classification and removal of EEG artifacts with SVM and wavelet-ICA, *IEEE Journal of Biomedical and Health Informatics* 22 (3) (2017) 664–670.
- [65] E. Estrada, H. Nazeran, G. Sierra, F. Ebrahimi, S.K. Setarehdan, Wavelet-based EEG denoising for automatic sleep stage classification, *International Conference on Electrical Communications and Computers* (2011) 295–298.
- [66] M. Unser, A. Aldroubi, A review of wavelets in biomedical applications, *Proc. IEEE* 84 (4) (1996) 626–638.
- [67] N.E. Huang, Z. Shen, S.R. Long, M.C. Wu, H.H. Shih, Q. Zheng, N.C. Yen, C. C. Tung, H.H. Liu, The empirical mode decomposition and the Hilbert spectrum for nonlinear and non-stationary time series analysis, *Proceedings of the Royal Society of London. Series A: Math. Phys. Eng. Sci.* 454 (1971) 903–995, 1998.
- [68] D. Iatsenko, P.V.E. McClintock, A. Stefanovska, Nonlinear mode decomposition: a noise-robust, adaptive decomposition method, *Phys. Rev. E* 92 (3) (2015) 032916.
- [69] P. Sawangjai, M. Trakulruangroj, C. Boonmag, M. Piriyajitakonkij, R.K. Tripathy, T. Sudhawiyangkul, T. Wilaprasitporn, EEGANet: removal of ocular artifacts from the EEG signal using generative adversarial networks, *IEEE Journal of Biomedical and Health Informatics* 26 (10) (2022) 4913–4924.
- [70] H.M. Zhang, M.Q. Zhao, C. Wei, D. Mantini, Z.R. Li, Q.Y. Liu, EEGdenoiseNet: a benchmark dataset for deep learning solutions of EEG denoising, *J. Neural. Eng.* 18 (5) (2021) 056057.
- [71] B.M. Wilamowski, N.J. Cotton, O. Kaynak, G. Dundar, Computing gradient vector and Jacobian matrix in arbitrarily connected neural networks, *IEEE Trans. Ind. Electron.* 55 (10) (2008) 3784–3790.
- [72] T.W. Sun, Y.P. Su, W. Xia, X.J. Wu, A novel end-to-end 1D-ResCNN model to remove artifact from EEG signals, *Neurocomputing* 404 (2020) 108–121.
- [73] S. Hochreiter, J. Schmidhuber, Long short-term memory, *Neural Comput.* 9 (8) (1997) 1735–1780.
- [74] T.F. Gao, D. Chen, Y.B. Tang, Z.K. Ming, X.L. Li, EEG reconstruction with a dual-scale CNN-LSTM model for deep artifact removal, *IEEE Journal of Biomedical and Health Informatics* 27 (3) (2023) 1283–1294.
- [75] A. Narmada, M.K. Shukla, A Novel Adaptive Artifacts Wavelet Denoising for EEG Artifacts Removal Using Deep Learning with Meta-Heuristic Approach, *Multimedia Tools and Applications*, 2023, pp. 1–39.
- [76] J.Y. Zhu, T. Park, P. Isola, A.A. Efros, Unpaired Image-To-Image Translation Using Cycle-Consistent Adversarial Networks, *IEEE International Conference on Computer Vision*, 2017, pp. 2223–2232.
- [77] G. Huang, *EEG/ERP Data Analysis Toolboxes*, Springer, Singapore, 2019, pp. 407–434.
- [78] A. Delorme, S. Makeig, EEGLAB: an open source toolbox for analysis of single-trial EEG dynamics including independent component analysis, *J. Neurosci. Methods* 134 (1) (2004) 9–21.
- [79] A. Gramfort, M. Luessi, E. Larson, D.A. Engemann, D. Strohmeier, C. Brodbeck, L. Parkkonen, M.S. Hämäläinen, MNE software for processing MEG and EEG data, *Neuroimage* 86 (1) (2014) 446–460.
- [80] R. Oostenveld, P. Fries, E. Maris, J.M. Schoffelen, FieldTrip: Open Source Software for Advanced Analysis of MEG, EEG, and Invasive Electrophysiological Data, *Computational Intelligence and Neuroscience*, 2011, pp. 1–9.
- [81] D.P. Subha, P.K. Joseph, U.R. Acharya, C.M. Lim, EEG signal analysis: a survey, *J. Med. Syst.* 34 (2) (2008) 195–212.
- [82] T. Gasser, P. Bächer, J. Möcks, Transformations towards the normal distribution of broad band spectral parameters of the EEG, *Electroencephalogr. Clin. Neurophysiol.* 53 (1) (1982) 119–124.
- [83] L.R. Quitadamo, R. Mai, F. Gozzo, V. Pelliccia, F. Cardinale, S. Seri, Kurtosis-based detection of intracranial high-frequency oscillations for the identification of the seizure onset zone, *International Journal of Neural Systems* 28 (7) (2018) 1850001.
- [84] B. Hjorth, EEG analysis based on time domain properties, *Electroencephalogr. Clin. Neurophysiol.* 29 (3) (1970) 306–310.
- [85] T. Inouye, K. Shinosaki, H. Sakamoto, S. Toi, S. Ukai, A. Iyama, Y. Katsuda, M. Hirano, Quantification of eeg irregularity by use of the entropy of the power spectrum, *Electroencephalogr. Clin. Neurophysiol.* 79 (3) (1991) 204–210.
- [86] H. Chao, L. Dong, Emotion recognition using three-dimensional feature and convolutional neural network from multichannel EEG signals, *IEEE Sensor. J.* 21 (2) (2020) 2024–2034.
- [87] S. Thapaliya, S. Jayarathna, M. Jaime, Evaluating the EEG and Eye Movements for Autism Spectrum Disorder, *IEEE International Conference on Big Data*, 2018, pp. 2328–2336.
- [88] T. Heunis, C. Aldrich, J.M. Peters, S.S. Jeste, M. Sahin, C. Scheffer, P.J. de Vries, Recurrence quantification analysis of resting state eeg signals in autism spectrum disorder-a systematic methodological exploration of technical and demographic confounders in the search for biomarkers, *BMC Med.* 16 (1) (2018) 1–17.
- [89] J.J. Esqueda-Elizondo, R. Juárez-Ramírez, O.R. López-Bonilla, E.E. García-Guerrero, G.M. Galindo-Aldana, L. Jiménez-Beristáin, A. Serrano-Trujillo, E. Tlelo-Cuautle, E. Inzunza-González, Attention measurement of an autism spectrum disorder user using EEG signals: a case study, *Math. Comput. Appl.* 27 (2) (2022) 21.
- [90] K.J. Friston, Functional and effective connectivity in neuroimaging: a synthesis, *Hum. Brain Mapp.* 2 (1–2) (1994) 56–78.
- [91] J. Geweke, Measurement of linear dependence and feedback between multiple time series, *J. Am. Stat. Assoc.* 77 (378) (1982) 304–313.
- [92] P. Fries, Rhythms for cognition: communication through coherence, *Neuron* 88 (1) (2015) 220–235.
- [93] J.P. Lachaux, E. Rodriguez, J. Martinerie, F.J. Varela, Measuring phase synchrony in brain signals, *Hum. Brain Mapp.* 8 (4) (1999) 194–208.
- [94] S. Aydore, D. Pantazis, R.M. Leahy, A note on the phase locking value and its properties, *Neuroimage* 74 (2013) 231–244.
- [95] C.C. French, J.G. Beaumont, A critical review of EEG coherence studies of hemisphere function, *Int. J. Psychophysiol.* 1 (3) (1984) 241–254.
- [96] D. Cordes, V.M. Haughton, K. Arfanakis, J.D. Carew, P.A. Turski, C.H. Moritz, M. A. Quigley, M.E. Meyerand, Frequencies contributing to functional connectivity in the cerebral cortex in “resting-state” data, *Am. J. Neuroradiol.* 22 (7) (2001) 1326–1333.
- [97] K. Pearson, Mathematical contributions to the theory of evolution - III. Regression, heredity, and panmixia, *Philos. Trans. R. Soc. Lond. - Ser. A Contain. Pap. a Math. or Phys. Character* 187 (1896) 253–318.
- [98] Z.J. Peña, M.A.H. Akhand, J.F. Srabonee, N. Siddique, EEG based autism detection using CNN through correlation based transformation of channels' Data, in: *2020 IEEE Region 10 Symposium*, 2020, pp. 1278–1281.
- [99] E. Bullmore, O. Sporns, Complex brain networks: graph theoretical analysis of structural and functional systems, *Nat. Rev. Neurosci.* 10 (3) (2009) 186–198.
- [100] T. Wadhera, M. Mahmud, Brain functional network topology in autism spectrum disorder: a novel weighted hierarchical complexity metric for electroencephalogram, *IEEE Journal of Biomedical and Health Informatics* 27 (4) (2023) 1718–1725.
- [101] R.D. Pascual-Marqui, C.M. Michel, D. Lehmann, Segmentation of brain electrical activity into microstates: model estimation and validation, *IEEE (Inst. Electr. Electron. Eng.) Trans. Biomed. Eng.* 42 (7) (1995) 658–665.
- [102] P. Milz, P.L. Faber, D. Lehmann, T. Koenig, K. Kochi, R.D. Pascual-Marqui, The functional significance of EEG microstates-Associations with modalities of thinking, *Neuroimage* 125 (15) (2016) 643–656.
- [103] A. Bochet, H.F. Sperdin, T.A. Rihs, N. Kojovic, M. Franchini, R.K. Jan, C. M. Michel, M. Schaefer, Early alterations of large-scale brain networks temporal dynamics in young children with autism, *Commun. Biol.* 4 (2020) 968.
- [104] D.F. D'Croz-Baron, M. Baker, C.M. Michel, T. Karp, EEG microstates analysis in young adults with autism spectrum disorder during resting-state, *Front. Hum. Neurosci.* 13 (2019) 000173.
- [105] X.L. Kong, J. Li, G.X. Ouyang, EEG Microstate Analysis for Diagnosis of Children with ASD, *42nd Chinese Control Conference*, 2023, pp. 3390–3395.
- [106] C.M. Michel, T. Koenig, EEG microstates as a tool for studying the temporal dynamics of whole-brain neuronal networks: a review, *Neuroimage* 180 (2018) 577–593.
- [107] J.N. Kang, T.Y. Zhou, J.X. Han, X.L. Li, EEG-based multi-feature fusion assessment for autism, *J. Clin. Neurosci.* 56 (2018) 101–107.
- [108] J.W. Cooley, J.W. Tukey, An algorithm for the machine calculation of complex Fourier series, *Math. Comput.* 19 (90) (1965) 297–301.
- [109] E. Neuhaus, S.J. Lowry, M. Santhosh, Resting state EEG in youth with ASD: age, sex, and relation to phenotype, *J. Neurodev. Disord.* 13 (1) (2021) 1–15.
- [110] J. Wang, X.M. Wang, X.L. Wang, H.Y. Zhang, Y. Zhou, L. Chen, Y.T. Li, L.J. Wu, Increased EEG coherence in long-distance and short-distance connectivity in children with autism spectrum disorders, *Brain and Behavior* 10 (10) (2020) e01796.
- [111] C. Bingham, M. Godfrey, J.W. Tukey, Modern techniques of power spectrum estimation, *IEEE Trans. Audio Electroacoust.* 15 (2) (1967) 56–66.
- [112] M. Ranjani, P. Supraja, Classifying the autism and epilepsy disorder based on EEG signal using deep convolutional neural network (DCNN), in: *International Conference on Advance Computing and Innovative Technologies in Engineering*, 2021, pp. 880–886.
- [113] N. Alotaibi, K. Maharatna, Classification of autism spectrum disorder from EEG-based functional brain connectivity analysis, *Neural Comput.* 33 (7) (2021) 1914–1941.
- [114] A.S. Al-Fahoum, A.A. Al-Fraihat, Methods of EEG Signal Features Extraction Using Linear Analysis in Frequency and Time-Frequency Domains, *International Scholarly Research Notices*, 2014 730218.
- [115] Z.G. Zhang, Spectral and Time-Frequency Analysis, *EEG Signal Processing and Feature Extraction*, 2019, pp. 89–116.
- [116] D. Griffin, J. Lim, Signal estimation from modified short-time Fourier transform, *IEEE Trans. Acoust. Speech Signal Process.* 32 (2) (1984) 236–243.
- [117] Z. Shi, X. Yang, Y. Li, G. Yu, Wavelet-based synchroextracting transform: an effective TFA tool for machinery fault diagnosis, *Control Eng. Pract.* 114 (2021) 104884.
- [118] K. Samiee, P. Kovacs, M. Gabbouj, Epileptic seizure classification of EEG time-series using rational discrete short-time Fourier transform, *IEEE (Inst. Electr. Electron. Eng.) Trans. Biomed. Eng.* 62 (2) (2014) 541–552.
- [119] M.N.A. Tawhid, S. Siuly, H. Wang, Diagnosis of autism spectrum disorder from EEG using a time-frequency spectrogram image-based approach, *Electron. Lett.* 56 (25) (2020) 1372–1375.
- [120] C.S. Burrus, R.A. Gopinath, H. Guo, J.E. Odegard, I.W. Selesnick, *Introduction to Wavelets and Wavelet Transforms-A Primer*, Prentice Hall, New Jersey, 1998.
- [121] F.F. Qi, W.L. Wang, X.F. Xie, Z.H. Gu, Z.L. Yu, F. Wang, Y.Q. Li, W. Wu, Single-trial eeg classification via orthogonal wavelet decomposition-based feature extraction, *Front. Neurosci.* 15 (2021) 715855.

- [122] M.N.A. Tawhid, S. Siuly, K.T. Wang, H. Wang, Automatic and efficient framework for identifying multiple neurological disorders from EEG signals, *IEEE Transactions on Technology and Society* 4 (1) (2023) 76–86.
- [123] S. Ibrahim, R. Djemal, A. Alsuailem, Electroencephalography (EEG) signal processing for epilepsy and autism spectrum disorder diagnosis, *Biocybern. Biomed. Eng.* 38 (1) (2018) 16–26.
- [124] M.T. Rosenstein, J.J. Collins, C.J. De Luca, A practical method for calculating largest Lyapunov exponents from small data sets, *Phys. Nonlinear Phenom.* 65 (1–2) (1993) 117–134.
- [125] F.A. Alturki, K. AlSharabi, A.M. Abdurraqeb, M. Aljalal, EEG signal analysis for diagnosing neurological disorders using discrete wavelet transform and intelligent techniques, *Sensors* 20 (9) (2020) 2505.
- [126] R. Djemal, K. AlSharabi, S. Ibrahim, A. Alsuailem, EEG-based computer aided diagnosis of autism spectrum disorder using wavelet, entropy, and ANN, *BioMed Res. Int.* (2017) 9816591.
- [127] D. Abdolzadegan, M.H. Moattar, M. Ghoshuni, A robust method for early diagnosis of autism spectrum disorder from EEG signals based on feature selection and DBSCAN method, *Biocybern. Biomed. Eng.* 40 (1) (2020) 482–493.
- [128] L.C. Cheong, R. Sudirman, S.S. Hussin, Feature extraction of EEG signal using wavelet transform for autism classification, *ARPEN J. Eng. Appl. Sci.* 10 (19) (2015) 8533–8540.
- [129] J.V. Hurtado, A. Valada, Semantic Scene Segmentation for Robotics, Deep Learning for Robot Perception and Cognition, Academic Press, 2022, pp. 279–311.
- [130] E. Abdulhay, M. Alafeef, H. Hadoush, V. Venkataraman, N. Arunkumar, EMD-based analysis of complexity with dissociated EEG amplitude and frequency information: a data-driven robust tool -for Autism diagnosis-compared to multi-scale entropy approach, *Math. Biosci. Eng.* 19 (5) (2022) 5031–5054.
- [131] S. Farahmand, T. Sobayo, D.J. Mogul, Noise-assisted multivariate EMD-based mean-phase coherence analysis to evaluate phase-synchronous dynamics in epilepsy patients, *IEEE Trans. Neural Syst. Rehabil. Eng.* 26 (12) (2018) 2270–2279.
- [132] G. Rilling, P. Flandrin, P. Goncalves, On empirical mode decomposition and its algorithms, *IEEE-EURASIP Workshop on Nonlinear Signal and Image Processing* 3 (3) (2003) 8–11.
- [133] P. Flandrin, G. Rilling, P. Goncalves, Empirical mode decomposition as a filter bank, *IEEE Signal Process. Lett.* 11 (2) (2004) 112–114.
- [134] J. Park, G.M. Pao, G. Sugihara, E. Stabenau, T. Lorimer, Empirical mode modeling: a data-driven approach to recover and forecast nonlinear dynamics from noisy data, *Nonlinear Dynam.* 3 (108) (2022) 2147–2160.
- [135] H. Hadoush, M. Alafeef, E. Abdulhay, Automated identification for autism severity level: EEG analysis using mode decomposition and second order difference plot, *Behav. Brain Res.* 362 (19) (2019) 240–248.
- [136] R.A. Thuraisingham, Y. Tran, P. Boord, A. Craig, Analysis of eyes open, eye closed EEG signals using second-order difference plot, *Med. Biol. Eng. Comput.* 45 (2007) 1243–1249.
- [137] E. Abdulhay, M. Alafeef, L. Alzghoul, M.A. Momani, R.A. Abdi, N. Arunkumar, R. Munoz, V.H.C. de Albuquerque, Computer-aided autism diagnosis via second-order difference plot area applied to EEG empirical mode decomposition, *Neural Comput. Appl.* 32 (2020) 10947–10956.
- [138] M.E. Cohen, D.L. Hudson, P.C. Deedwania, Applying continuous chaotic modeling to cardiac signal analysis, *IEEE Eng. Med. Biol. Mag.* 15 (5) (1996) 97–102.
- [139] L. Abou-Abbas, S. van Noortd, J.A. Desjardins, M. Cichonski, M. Elsabbagh, Use of empirical mode decomposition in ERP analysis to classify familial risk and diagnostic outcomes for autism spectrum disorder, *Brain Sci.* 11 (4) (2021) 409.
- [140] C. Cortes, V. Vapnik, Support-vector networks, *Mach. Learn.* 20 (1995) 273–297.
- [141] S. Amari, S. Wu, Improving support vector machine classifiers by modifying kernel functions, *Neural Networks* 12 (6) (1999) 783–789.
- [142] L. Breiman, Random forests, *Mach. Learn.* 45 (2001) 5–32.
- [143] W. Jamal, S. Das, I.A. Oprescu, K. Maharatna, F. Apicella, Classification of autism spectrum disorder using supervised learning of brain connectivity measures extracted from synchronostates, *J. Neural. Eng.* 11 (4) (2014) 046019.
- [144] E. Grossi, C. Olivieri, M. Buscema, Diagnosis of autism through EEG processed by advanced computational algorithms: a pilot study, *Comput. Methods Progr. Biomed.* 142 (2017) 73–79.
- [145] J.G. Attali, G. Pagès, Approximations of functions by a multilayer perceptron: a new approach, *Neural Network*. 10 (6) (1997) 1069–1081.
- [146] L.E. Peterson, K-nearest neighbor, *Scholarpedia* 4 (2) (2009) 1883.
- [147] Y.Y. Sun, Y.F. Ming, X.J. Zhu, Y.X. Li, Out-of-distribution detection with deep nearest neighbors, *international conference on machine learning*, *PMLR* 162 (2022) 20827–20840.
- [148] D.W. Hosmer Jr., S. Lemeshow, R.X. Sturdivant, *Applied Logistic Regression*, John Wiley & Sons, 2013.
- [149] S. Jayarathna, Y. Jayawardana, M. Jaime, S. Thapaliya, *Electroencephalogram (EEG) for Delineating Objective Measure of Autism Spectrum Disorder, Computational Models for Biomedical Reasoning and Problem Solving*, 2019, pp. 34–65.
- [150] Q.L. Li, R.F. Weiland, I. Konvalinka, H.D. Mansvelder, T.S. Andersen, D.J.A. Smit, S. Begeer, K. Linkenkaer - Hansen, Intellectually able adults with autism spectrum disorder show typical resting - state EEG activity, *Sci. Rep.* 12 (1) (2022) 19016.
- [151] S. Peketi, S.B. Dhok, Machine learning enabled P300 classifier for autism spectrum disorder using adaptive signal decomposition, *Brain Sci.* 13 (2) (2023) 315.
- [152] P. Wang, E. Fan, P. Wang, Comparative analysis of image classification algorithms based on traditional machine learning and deep learning, *Pattern Recogn. Lett.* 141 (2021) 61–67.
- [153] Y. Lecun, L. Bottou, Y. Bengio, P. Haffner, Gradient-based learning applied to document recognition, *Proc. IEEE* 86 (11) (1998) 2278–2324.
- [154] L. Alzubaidi, J.L. Zhang, A.J. Humaidi, A. Al-Dujaili, Y. Duan, O. Al-Shamma, J. Santamaría, M.A. Fadhel, M. Al-Amidie, Laith Farhan, Review of deep learning: concepts, CNN architectures, challenges, applications, future directions, *Journal of Big Data* 8 (2021) 53.
- [155] M.N.A. Tawhid, S. Siuly, H. Wang, F. Whittaker, K. Wang, Y.C. Zhang, A spectrogram image based intelligent technique for automatic detection of autism spectrum disorder from EEG, *PLoS One* 16 (6) (2021) e0253094.
- [156] B. Ari, N. Sobahi, Ö.F. Alçin, A. Sengür, U.R. Acharya, Accurate detection of autism using Douglas-Peucker algorithm, sparse coding based feature mapping and convolutional neural network techniques with EEG signals, *Comput. Biol. Med.* 143 (2022) 105311.
- [157] Q.M. Din, A.K. Jayanthi, Automated classification of autism spectrum disorder using EEG signal and convolutional neural networks, *Biomed. Eng.: Applications, Basis and Communications* 34 (2) (2022) 2250020.
- [158] C. Stamatte, G.D. Magoulas, M.S.C. Thomas, Deep learning topology-preserving EEG-based images for autism detection in infants, *Engineering Applications of Neural Networks Conference* 3 (2021) 71–82.
- [159] C. Szegedy, W. Liu, Y.Q. Jia, P. Sermanet, S. Reed, D. Anguelov, D. Erhan, V. Vanhoucke, A. Rabinovich, Going Deeper with Convolutions, *Computer Vision and Pattern Recognition*, 2015, pp. 1–9.
- [160] A. Krizhevsky, I. Sutskever, G.E. Hinton, Imagenet classification with deep convolutional neural networks, *Commun. ACM* 60 (6) (2017) 84–90.
- [161] A.G. Howard, M.J. Zhu, B. Chen, D. Kalenichenko, W.J. Wang, T. Weyand, M. Andreetto, H. Adam, MobileNets: Efficient Convolutional Neural Networks for Mobile Vision Applications, 2017 arXiv preprint arXiv:1704.04861.
- [162] F.N. Iandola, S. Han, M.W. Moskewicz, K. Ashraf, W.J. Dally, K. Keutzer, SqueezeNet: AlexNet-Level Accuracy with 50x Fewer Parameters and <0.5MB Model Size, 2016 arXiv preprint arXiv:1602.07360.
- [163] K.M. He, X.Y. Zhang, S.Q. Ren, J. Sun, Deep Residual Learning for Image Recognition, *IEEE Conference on Computer Vision and Pattern Recognition*, 2016, pp. 770–778.
- [164] J.L. Tan, Y.C. Zhan, Y. Tang, W.X. Bao, Y. Tian, EEG Decoding for Effects of Visual Joint Attention Training on ASD Patients with Interpretable and Lightweight Convolutional Neural Network, *Cognitive Neurodynamics*, 2023, pp. 1–14.
- [165] V.J. Lawhern, A.J. Solon, N.R. Waytowich, S.M. Gordon, C.P. Hung, B.J. Lance, EEGNet: a compact convolutional neural network for EEG-based brain-computer interfaces, *J. Neural. Eng.* 15 (5) (2018) 056013.
- [166] R.M. Peng, C.M. Zhao, J. Jiang, G.T. Kuang, Y.Q. Cui, Y.F. Xu, H. Du, J.B. Shao, D. R. Wu, TIE-EEGNet: temporal information enhanced EEGNet for seizure subtype classification, *IEEE Trans. Neural Syst. Rehabil. Eng.* 30 (2022) 2567–2576.
- [167] T. Wadhhera, D. Kakkar, R. Rani, Behavioral Modeling Using Deep Neural Network Framework for ASD Diagnosis and Prognosis, *Emerging Technologies for Healthcare: Internet of Things and Deep Learning Models*, 2021, pp. 279–298.
- [168] T.N. Kipf, M. Welling, Semi-supervised Classification with Graph Convolutional Networks, 2016 arXiv preprint arXiv:1609.02907.
- [169] H.Y. Dong, D. Chen, L. Zhang, H.J. Ke, X.L. Li, Subject sensitive EEG discrimination with fast reconstructable CNN driven by reinforcement learning: a case study of ASD evaluation, *Neurocomputing* 449 (18) (2021) 136–145.
- [170] D.E. Rumelhart, G.E. Hinton, R.J. Williams, Learning representations by back-propagating errors, *Nature* 323 (6088) (1986) 533–536.
- [171] N.A. Ali, A.R. Syafeeza, A.S. Jaafar, S. Shamsuddin, N.K. Nor, LSTM-based electroencephalogram classification on autism spectrum disorder, *International Journal of Integrated Engineering* 13 (6) (2021) 321–329.
- [172] N.A. Ali, A.R. Syafeeza, A.S. Jaafar, N.K. Nor, ConVnet BiLSTM for ASD classification on EEG brain signal, *International Journal of Online & Biomedical Engineering* 18 (11) (2022) 77–94.
- [173] Y.B. Tang, D. Chen, H.h. Liu, C. Cai, X.L. Li, Deep EEG superresolution via correlating brain structural and functional connectivities, *IEEE Trans. Cybern.* 53 (7) (2023) 1–13.
- [174] J.N. Kang, X.Y. Han, J.J. Song, Z.K. Niu, X.L. Li, The identification of ASD children spectrum disorder by SVM approach on EEG and eye-tracking data, *Comput. Biol. Med.* 120 (2020) 103722.
- [175] S.S. Zhang, D. Chen, Y.B. Tang, L. Zhang, Children ASD evaluation through joint analysis of EEG and Eye-tracking recordings with graph convolution network, *Front. Hum. Neurosci.* 15 (2021) 651349.
- [176] J.X. Han, G.Q. Jiang, G.X. Ouyang, X.L. Li, A Multi-modal approach for identifying autism spectrum disorders in children, *IEEE Trans. Neural Syst. Rehabil. Eng.* 30 (2022) 2003–2011.
- [177] S.S. Zhang, D. Chen, Y.B. Tang, X.L. Li, Learning graph-based relationship of dual-modal features towards subject adaptive ASD assessment, *Neurocomputing* 516 (7) (2023) 194–204.
- [178] M. Liao, H. Duan, G. Wang, Application of machine learning techniques to detect the children with autism spectrum disorder, *Journal of Healthcare Engineering* (2022) 9340027.
- [179] M. Baygin, S. Dogan, T. Tuncer, P.D. Barua, U.R. Acharya, Automated ASD detection using hybrid deep light-weight features extracted from EEG signals, *Comput. Biol. Med.* 134 (2021) 104548.
- [180] N.A. Ali, A.R. Syafeeza, A.S. Jaafar, M.K.M.F. Alif, Autism spectrum disorder classification on electroencephalogram signal using deep learning algorithm, *IAES Int. J. Artif. Intell.* 9 (1) (2022) 91–99.

- [181] T. Wadhera, M. Mahmud, Computing hierarchical complexity of the brain from electroencephalogram signals: a graph convolutional network-based approach, International Joint Conference on Neural Networks (2022) 1–6.
- [182] Q.M. ud-Din, A.K. Jayanthy, Wavelet scattering transform and deep learning networks based autism spectrum disorder identification using EEG signals, Trait. Du. Signal 39 (6) (2022) 2069–2076.
- [183] S.B. Moqadam, A.S. Asheghabadi, F. Norouzi, H. Jafarzadeh, A. Khosroabadi, A. Alagheband, G. Bangash, N. Morovatdar, J. Xu, Conceptual method of temperature sensation in bionic hand by extraordinary perceptual phenomenon, JBE 18 (2021) 1344–1357.